

New thiazolidinones reduce iron overload in mouse models of hereditary hemochromatosis and β -thalassemia

Jing Liu,^{1, 2, #} Wei Liu,^{1, 2, #} Yin Liu,^{1, 3} Yang Miao,¹ Yifan Guo,¹ Haoyang Song,¹ Fudi Wang,⁴ Hongyu Zhou,⁵ Tomas Ganz,⁶ Bing Yan^{3, 5} and Sijin Liu^{1, 2}

¹State Key Laboratory of Environmental Chemistry and Ecotoxicology, Research Center for Eco-Environmental Sciences, Chinese Academy of Sciences, Beijing, China; ²University of Chinese Academy of Sciences, Beijing, China; ³School of Environmental Science and Engineering, Shandong University, Shandong, China; ⁴Department of Nutrition, Nutrition Discovery Innovation Center, Institute of Nutrition and Food Safety, School of Public Health, School of Medicine, Zhejiang University, Zhejiang, China; ⁵Key Laboratory for Water Quality and Conservation of the Pearl River Delta, Ministry of Education, Institute of Environmental Research at Greater Bay, Guangzhou University, Guangzhou, China and ⁶Department of Medicine and Department of Pathology, David Geffen School of Medicine at University of California, California, Los Angeles, CA, USA

#JL and WL contributed equally to this work

©2019 Ferrata Storti Foundation. This is an open-access paper. doi:10.3324/haematol.2018.209874

Received: October 21, 2018.

Accepted: February 15, 2019.

Pre-published: February 21, 2019.

Correspondence: BING YAN - drbingyan@yahoo.com

SIJIN LIU - sjliu@rcees.ac.cn

Supplementary information

New thiazolidinones reduce iron overload in mouse models of hereditary hemochromatosis and β -thalassemia

Jing Liu^{1, 2, #}, Wei Liu^{1, 2, #}, Yin Liu^{1, 3}, Yang Miao¹, Yifan Guo¹, Haoyang Song¹, Fudi Wang⁴,
Hongyu Zhou⁵, Tomas Ganz⁶, Bing Yan^{3, 5*}, Sijin Liu^{1, 2,*}

1. State Key Laboratory of Environmental Chemistry and Ecotoxicology, Research Center for Eco-Environmental Sciences, Chinese Academy of Sciences, Beijing 100085, China
2. University of Chinese Academy of Sciences, Beijing, 100049, P. R. China
3. School of Environmental Science and Engineering, Shandong University, Shandong, 250100, China
4. Department of Nutrition, Nutrition Discovery Innovation Center, Institute of Nutrition and Food Safety, School of Public Health, School of Medicine, Zhejiang University, Zhejiang, 310058, China
5. Key Laboratory for Water Quality and Conservation of the Pearl River Delta, Ministry of Education, Institute of Environmental Research at Greater Bay, Guangzhou University, Guangzhou, 510006, China
6. Department of Medicine and Department of Pathology, David Geffen School of Medicine at University of California Los Angeles, CA, 90095, USA

*: Correspondence to Drs. Bing Yan (email: drbingyan@yahoo.com) and Sijin Liu (email: sjliu@rcees.ac.cn).

#Jing Liu and Wei Liu contributed equally to this work.

Abbreviation

FPN	Ferroportin
HH	Hereditary hemochromatosis
HFE	Hemochromatosis
DFO	Desferrioxamine
qRT-PCR	Quantitative RT-PCR
IL-6	Interleukin 6
TNF- α	Tumor necrosis factor- α
EPO	Erythropoietin
LDH	Lactate dehydrogenase
AST	Aspartate aminotransferase
ALT	Alanine aminotransferase
CBC	Complete blood count
<i>I.P.</i>	Intraperitoneal
Wt	Wildtype
LPS	Lipopolysaccharide
SAA1	Serum amyloid A1
P-SMAD1/5/8	Phosphorylated SMAD1/5/8
TMPRSS6	Transmembrane protease serine 6
ID1	Inhibitor of DNA binding
SMAD7	SMAD family member 7
TFR2	Transferrin receptor 2
HJV	Hemojuvelin
BMPRs	Bone morphogenetic protein receptors
P-ERK1/2	Phosphorylated ERK1/2
GDF15	Growth differentiation factor 15
TWSG1	Twisted gastrulation BMP signaling modulator 1
ERFE	Erythroferrone
<i>Hamp1</i> ^{-/-}	Hepcidin deficient
<i>Hfe</i> ^{-/-}	HFE deficient
HGB	Haemoglobin
RBC	Red blood cell
MDA	Malondialdehyde
ROS	Reactive oxygen species

Supplemental Methods

Cell culture

Human SMMC-7721 and mouse Hepa 1-6 cell line were obtained from the Shanghai Cell Bank of Type Culture Collection of the Chinese Academy of Sciences (Shanghai, China). Cells were cultured in RPMI 1640 medium (Gibco, USA), supplemented with 10% fetal bovine serum (FBS, Gibco, USA) and 100 U/mL penicillin–streptomycin (Corning, USA) at 37 °C and under 5% CO₂.

Luciferase reporter assay

Briefly, 1×10^4 cells were seeded in 96-well plates 12 h prior to plasmid transfection. SMMC-7721 cells were co-transfected with 0.2 µg hepcidin firefly plasmid¹ and 20 ng renilla luciferase plasmid using Lipofectamine™ 2000 (Invitrogen, USA). After 24 h, cells were washed with cold PBS, and were then subjected to cellular lysis in lysis buffer (Promega, USA). Cell lysates were assayed for luciferase activities using a dual-luciferase reporter assay kit (Promega, USA). Firefly luciferase activities were normalized to those of renilla luciferase for quantification.

RNA extraction and quantitative RT-PCR (qRT-PCR)

Total RNAs were purified from tissue specimens or cells using Trizol reagent following the manufacturer's instruction (Invitrogen, USA). The relative expression levels for target genes were determined by qRT-PCR, using SYBR Green qPCR mix (Promega) on a Mx3005P qRT-PCR instrument (Bio-Rad, USA). Primers used in the current study are listed in Table S1. *Gapdh* was used as an internal control.

Animal experimentation

All animal experiments were approved by the Animal Ethics Committee at Research Center for Eco-Environmental Sciences, Chinese Academy of Sciences. Balb/C mice were purchased from the Laboratory Animal Technology Co., Ltd (Beijing, China). Hcpidin-knockout mice under C57BL/6 background were originally provided by Dr. Sophie Vaultont² and Dr. Tomas Ganz³. *Hfe*^{-/-} mice on the 129S background were provided by Dr. Fudi Wang⁴. *Hbb*^{th3/+} mice (the Jackson Laboratory) on C57BL/6 background were used as a β -thalassemia intermedia model⁵. All mice were bred in a specific pathogen-free (SPF) facility. Compounds were dissolved in stock solution (5.7% DMSO, 9.6% Cremophor EL and 9.6% ethanol in PBS) and were injected by the intraperitoneal route at a dose of 2, 10 and 30 mg/kg per body weight. Mice were sacrificed at different time points after treatment, peripheral blood was collected, and organs were harvested for further experiments.

Determination of hepcidin, transferrin, cytokine and amino-transaminase

Serum hepcidin, transferrin and ferritin levels were measured by ELISA assay kits purchased from USCN (Wuhan, China). We also used ELISA kits for serum interleukin 6 (IL-6) and tumor necrosis factor- α (TNF- α) (Origene, USA) and erythropoietin (EPO) (Solarbio, China). Levels of lactate dehydrogenase (LDH) (Nanjing Jiancheng Bioengineering Institute, China), aspartate aminotransferase (AST) and alanine aminotransferase (ALT) (Shanghai QiaoDu Biotechnology, China) in sera were measured with kits following instructions from the manufacturers.

Western blot analysis

Total proteins were first extracted from tissue specimens or cells with RIPA lysis buffer (Solarbio, China) containing 15% proteinase inhibitor cocktail (Roche). The concentrations of total proteins were determined with the Lowry method. Afterwards, the same amounts of total

proteins (20-100 µg) were subjected to 10% SDS-PAGE (Bio-Rad), followed by blotting analysis, as previously described⁶. The primary antibodies (Abs) were as follows, phosphorylated-SMAD1/5/8 (1:1000, Cell Signaling Technology (CST), USA), Smad1 (1:1000, CST), phosphorylated-ERK1/2 (1:1000, CST), ERK1 (1:1000, Proteintech, China), TMPRSS6 (1:1000, Proteintech, China) and GAPDH (1: 1000, Santa Cruz Biotechnology, USA).

Assay for iron parameters

Serum iron concentration was determined with a kit following the protocol from the manufacturer (Nanjing Jiancheng Bioengineering Institute, China). Hepatic and splenic non-heme iron content were assessed according to established methods⁷. Briefly, liver and spleen specimens were ultra-sonicated in an ultrasonic instrument with cubic zirconia beads, and were then incubated with the acid solution (49.6% HCl, 20% saturated trichloroacetic acid, 30.4% H₂O, v/v/v) at 65°C for 72 h. Iron concentration of each sample was measured by Chromagen solution. The absorbance at 535 nm was recorded with a VarioskanTM Flash multimode reader (Thermo Fisher Scientific, USA).

Histological examination and iron staining

Tissue specimens were first fixed in 10% PBS-buffered formaldehyde, and were then embedded in paraffin, followed by sectioning and hematoxylin-eosin (H&E) staining. Deparaffinized tissue sections were treated with 1% hydrogen peroxide (H₂O₂) for 10 min to eliminate the activity of endogenous peroxidase. Tissue sections were stained with Perls Prussian blue (blue stain) or DAB-enhanced Perls stain (brown stain) (Solarbio, China), following a standard protocol⁸. Slides were counter-stained with eosin (Sigma-Aldrich, USA).

Complete blood count (CBC) analysis

Peripheral blood was collected through heart puncture, and 20 μ L fresh blood was diluted into 2 mL standard dilution buffer provided by the manufacturer (Nihon Kohden, Japan). The diluted samples were then analyzed on a hematology analyzer (Nihon Kohden). Serum was separated from peripheral blood for further determinations.

Flow cytometry analysis

Erythropoiesis profile was defined based on expression levels of TER119 and CD44 and cellular size using an established method⁹. Briefly, bone marrow and spleen cells were first blocked with TruStain fcXTm (anti-mouse CD16/32 Ab, Biolegend, USA) in PBS with 0.5% bovine serum albumin (BSA) in ice for 10 min, and then stained with FITC-conjugated anti-mouse TER119 and PE-conjugated anti-mouse CD44 Abs (Biolegend, USA) in ice for 20 min in the dark. Afterwards, cells were washed and analyzed on a LSR II Flow Cytometer (BD, USA).

Supplementary Figure Legend

Figure S1. Chemical structure of synthesized thiazolidinone library. Representative structures of building blocks from anilines (R_1 in red) and aromatic aldehydes (R_2 in blue) were also shown.

Figure S2. Cell viability of SMMC-7721 cells after compound treatment.

After compound treatment at (A) 10 μ M and (B) 50 μ M for 24 h, the cell viability was measured by the MTT assay.

Figure S3. Hepcidin and serum iron changes in mice following compound administration.

(A) The variation of hepatic hepcidin mRNA expression in Wt Balb/C mice 6 and 24 h after

I.P. injection at 30 mg/kg body weight (n=4-6). (B) Changes of serum hepcidin and serum iron in Balb/C mice after *I.P.* injection for 6 and 24 h (n=4-6). *: P<0.05, and #: P<0.001, compared to untreated control.

Figure S4. Hepatic hepcidin mRNA expression in Wt Balb/C mice.

The changes of hepatic hepcidin mRNA expression in Wt Balb/C mice 24 h after *I.P.* injection at various concentrations (n=4-6). *: P<0.05, compared to untreated mice.

Figure S5. Time-course changes of hepcidin and iron parameters in Balb/C mice treated with compounds at 10 mg/kg body weight.

(A) Relative hepatic hepcidin mRNA expression determined by qRT-PCR (n=4-6). Levels of (B) serum iron, (C) splenic iron and (D) hepatic iron in Balb/C mice were measured at 10 mg/kg body weight after different time-course treatments (n=4-6). *: P<0.05; #: P<0.001, relative to untreated mice.

Figure S6. Histological examination of organs.

H&E staining of liver, spleen, kidney, lung, heart and bone marrow sections in Wt mice following **93**, **156** and **165** administration for (A) single dose after 24 h and (B) six doses after 12 days. Original magnification, ×100.

Figure S7. Injury and inflammation markers in Wt mice after compound administration.

Serum (A) AST, (B) ALT and (C) LDH levels in mice following compound administration at 30 mg/kg body weight for 24 h and 12 days (n=4). (D) Serum IL-6 were monitored at 24 h and 12 days (n=4). (E) Hepatic *Saa1* was detected at 6 and 24 h after compound administration (n=4). (F) Serum TNF- α concentration was determined 24 h and 12 days after **93**, **156** and **165** administration (n=4). *: P<0.05; #: P<0.001, relative to untreated mice.

Figure S8. CBC analysis in Wt mice upon compound administration.

After compound administration at 30 mg/kg body weight, CBC was detected for (A) 24 h and (B) 12 days (n=4).

Figure S9. Changes of EPO and erythroid regulators after treatment with compounds.

Changes of serum EPO concentrations in Balb/C mice after compound administration for 24 and 48 h.

Figure S10. Iron status in *Hamp*^{-/-} mice after 93, 156 and 165 administration.

(A) The experimental scheme of *Hamp*^{-/-} mice. Changes of (B) serum iron, (C) hepatic iron and (D) splenic iron in *Hamp*^{-/-} mice 6 and 24 h after 93, 156 and 165 administration at 30 mg/kg body weight (n=4).

Figure S11. Heparin and iron levels in untreated 4-, 6-, 8- and 10-week-old Wt 129S mice and *Hfe*^{-/-} mice.

(A) Relative hepatic hepcidin expression determined by qRT-PCR. Levels of (B) serum iron, (C) hepatic iron and (D) splenic iron were assayed (n=4). *: P<0.05; #: P<0.001, relative to untreated *Hfe*^{-/-} mice.

Figure S12. Iron parameters of 5-week-old *Hfe*^{-/-} mice after compound administration.

Changes of (A) splenic iron, (B) transferrin saturation and (C) serum ferritin and (D) serum transferrin of 5-week-old *Hfe*^{-/-} mice treated with 93, 156 and 165 at 10 mg/kg body weight every other day for 2 weeks (n=4-6). *: P<0.05, compared to untreated control; #: P<0.001, compared to untreated control.

Figure S13. Lack of inflammation and tissue injuries after 10 mg/kg body weight

compound administration in 5-week-old *Hfe*^{-/-} mice.

Serum (A) IL-6, (B) AST, (C) ALT and (D) LDH changes in 5-week-old *Hfe*^{-/-} mice treated with **93**, **156** and **165** at 10 mg/kg body weight for 2 weeks (n=4).

Figure S14. Serum hepcidin and iron parameters of 5-week-old *Hfe*^{-/-} mice after 93 administration for 4 weeks.

Changes of (A) serum hepcidin, (B) serum iron, (C) hepatic iron and (D) splenic iron after compound **93** administration at 10 mg/kg body weight every other day for 4 weeks (n=4-6). (E) Iron staining (in blue) of liver and spleen sections from these mice (original magnification, ×200 for liver, and ×100 for spleen). *: P<0.05, relative to untreated *Hfe*^{-/-} mice.

Figure S15. Inflammation and liver injury makers in 5-week-old *Hfe*^{-/-} mice after 4-week 93 administration.

Changes of serum (A) IL-6, (B) AST and (C) ALT concentrations in *Hfe*^{-/-} mice after **93** administration at 10 mg/kg every other day for 4 weeks.

Figure S16. Compound administration in iron-depleted *Hfe*^{-/-} mice.

Changes of (A) transferrin saturation and (B) serum transferrin levels of 9-week-old *Hfe*^{-/-} mice with pre-iron depletion for 4 weeks responding to **93**, **156** and **165** at 30 mg/kg body weight for another two weeks (n=4-6). *: P<0.05; #: P<0.001, relative to untreated *Hfe*^{-/-} mice.

Figure S17. Lack of inflammation and tissue injury in 5-week-old iron-depleted *Hfe*^{-/-} mice after 30 mg/kg compound administration.

Serum (A) IL-6, (B) AST and (C) ALT concentrations in the low-iron diet model of 9-week-old *Hfe*^{-/-} mice upon **93**, **156** and **165** at 30 mg/kg body weight for two weeks (n=4).

Figure S18. Erythropoiesis in *Hbb*^{th3/+} mice after treatment with compound 93, 156 and

165.

(A) Flow cytometry analysis of erythropoiesis in spleen cells from 4-week-old *Hbb^{th3/+}* mice following compound administration at 10 mg/kg body weight every other day for 2 weeks (n=3-4).

Figure S19. Serum hepcidin and iron parameters of *Hbb^{th3/+}* mice upon compound 93 administration for 4 weeks.

Changes of (A) serum hepcidin, (B) serum iron, (C) hepatic iron and (D) splenic iron in *Hbb^{th3/+}* mice after 93 administration at 10 mg/kg body weight for 4 weeks. (E) Iron staining of liver and spleen sections (in blue) from *Hbb^{th3/+}* mice through Perls Prussian staining, and liver iron staining was enhanced by DAB (in brown. Original magnification, ×400 for liver specimens, and ×200 for spleen specimens. (F) Spleen images and (G) the ratio of spleen weight/body weight of *Hbb^{th3/+}* mice after 93 administration for 4 weeks in comparison to untreated *Hbb^{th3/+}* mice. *: P<0.05; #: P<0.001, relative to untreated *Hbb^{th3/+}* mice.

Figure S20. Erythropoiesis in *Hbb^{th3/+}* mice after treatment with 93 for 4 weeks.

Changes of (A) HGB and (B) RBC levels of *Hbb^{th3/+}* mice upon 93 administration every other day for 4 weeks at 10 mg/kg body weight. (C) Blood smear (original magnification, ×1000) (damaged or deformed erythrocytes were denoted by red arrows) and (D) representative erythropoiesis profiles of bone marrow cells and spleen cells in *Hbb^{th3/+}* mice after 93 treatment. *: P<0.05, relative to untreated *Hbb^{th3/+}* mice.

Figure S21. Splenic MDA in *Hbb^{th3/+}* mice upon 93 administration

Changes of splenic MDA in *Hbb^{th3/+}* mice upon 93 administration at 10 mg/kg body weight for 4 weeks. #: P<0.001, compared to untreated mice.

Figure S22. EPO concentration in *Hbb*^{th3/+} mice upon compound 93 administration.

Serum EPO level in *Hbb*^{th3/+} mice after **93** treatment at 10 mg/kg for 4 weeks.

Table S1. Primer sequences used in the current study.

Interest genes	Primer sequences	
Human- <i>Gapdh</i>	F	5'-GAAGGTGAAGGTCGGAGT-3'
	R	5'-GAAGATGGTGATGGGATTTC-3'
Human - <i>Hepcidin</i>	F	5'-CACATCCCACACTTTGATCG-3'
	R	5'-CTGAGCAGCACCCACCTATCTC-3'
Mouse- <i>Gapdh</i>	F	5'-AAGGTCATCCCAGAGCTG-3'
	R	5'-GCCATGAGGTCCACCACCCT-3'
Mouse - <i>Hepcidin</i>	F	5'-CTGAGCAGCACCCACCTATCTC-3'
	R	5'-TGGCTCTAGGCTATGTTTTGC-3'
Mouse - <i>Id1</i>	F	5'- ACCCTGAACGGCGAGATCA-3'
	R	5'- TCGTCGGCTGGAACACATG-3'
Mouse - <i>Smad7</i>	F	5'- GCAGGCTGTCCAGATGCTGT-3'
	R	5'- GATCCCCAGGCTCCAGAAGA-3'
Mouse- <i>Saa1</i>	F	5'-AGTCTGGGCTGCTGAGAAAA-3'
	R	5'-ATGTCTGTTGGCTTCCTGTG-3'

Table S2. Structure information and R1/R2 group annotations of tested compounds.

	R1	R2	MW
1	H	H	280.07
2	H	Furan-2-yl	270.05
3	H	3-Methoxy-4-hydroxyl	326.07
4	H	3-Nitro	325.05
5	H	4-Methoxy	310.08
6	H	4-Phenyl	356.10
7	H	4-Cyano	305.06
8	H	4-Naphthalen-2-yl	330.08
9	H	4-Carboxyl	324.06
10	H	4-Acetamido	337.09
11	H	4-Carboxymethoxyl	354.07
12	2-Me	H	294.08
13	2-Me	3-Methoxy-4-hydroxyl	340.09
14	2-Me	3-Nitro	339.07
15	2-Me	2-hydroxyl	310.08
16	2-Me	2-Cl	328.04
17	2-Me	4-Formyl	322.08
18	2-Me	4-Phenyl	370.11
19	2-Me	4-Cyano	319.08
20	2-Me	4-Naphthalen-2-yl	344.10
21	2-Me	2,4,5-Trimethoxyl	384.11
22	2-Me	9H-Fluoren-2-yl	382.11
23	2-Me	4-Methylthio	340.07
24	2-Me	4-Acetamido	351.10
25	2-Me	4-Carboxymethoxyl	368.08
26	4-Me	H	294.08
27	4-Me	Furan-2-yl	284.06
28	4-Me	3-Methoxy-4-hydroxyl	340.09
29	4-Me	3-Nitro	339.07
30	4-Me	4-Methoxy	324.09
31	4-Me	2-hydroxyl	310.08
32	4-Me	2-Cl	328.04
33	4-Me	4-Formyl	322.08
34	4-Me	4-Cyano	319.08
35	4-Me	4-Naphthalen-2-yl	344.10
36	4-Me	2,4,5-Trimethoxyl	384.11
37	4-Me	9H-Fluoren-2-yl	382.11
38	4-Me	4-Methylthio	340.07
39	4-Me	4-Acetamido	351.10
40	2-Cl	3-Methoxy-4-hydroxyl	360.03
41	2-Cl	3-Nitro	359.01

42	2-Cl	4-Methoxy	344.04
43	2-Cl	4-Formyl	342.02
44	2-Cl	4-Phenyl	390.06
45	2-Cl	4-Naphthalen-2-yl	364.04
46	2-Cl	4-Carboxyl	358.02
47	2-Cl	2,4,5-Trimethoxyl	404.06
48	2-Cl	9H-Fluoren-2-yl	402.06
49	2-Cl	4-Methylthio	360.02
50	2-Cl	4-Acetamido	371.05
51	4-Cl	Furan-2-yl	304.01
52	4-Cl	3-Methoxy-4-hydroxyl	360.03
53	4-Cl	9H-Fluoren-2-yl	402.06
54	4-Cl	4-Methylthio	360.02
55	2-MeO	4-Phenyl	386.11
56	2-MeO	4-Naphthalen-2-yl	360.09
57	2-MeO	4-Carboxyl	354.07
58	2-MeO	2,4,5-Trimethoxyl	400.11
59	2-MeO	9H-Fluoren-2-yl	398.11
60	2-MeO	4-Methylthio	356.07
61	2-MeO	4-Acetamido	367.10
62	3-NO ₂	H	325.05
63	3-NO ₂	Furan-2-yl	315.03
64	3-NO ₂	3-Methoxy-4-hydroxyl	371.06
65	3-NO ₂	3-Nitro	370.04
66	3-NO ₂	4-Carboxymethoxyl	384.08
67	3-NO ₂	2-hydroxyl	341.05
68	3-NO ₂	4-Dimethylamino	368.09
69	3-NO ₂	2-Cl	359.01
70	3-NO ₂	4-Formyl	353.05
71	3-NO ₂	4-Phenyl	401.08
72	3-NO ₂	9H-Fluoren-2-yl	413.08
73	3-NO ₂	4-Methylthio	371.04
74	4-Acetyl	Furan-2-yl	312.06
75	4-Acetyl	3-Methoxy-4-hydroxyl	368.08
76	4-Acetyl	2-Hydroxyl	338.07
77	4-Acetyl	2,4,5-Trimethoxyl	412.11
78	3-CF ₃	H	348.05
79	3-CF ₃	2-Hydroxyl	
80	3-CF ₃	3-Nitro	393.06
81	3-CF ₃	4-Methoxy	378.07
82	3-CF ₃	2-hydroxyl	364.05
83	3-CF ₃	4-Dimethylamino	391.10
84	3-CF ₃	4-Phenyl	424.09
85	3-CF ₃	4-Naphthalen-2-yl	398.07
86	3-CF ₃	4-Carboxyl	392.04
87	3-CF ₃	2,4,5-Trimethoxyl	438.09
88	3-CF ₃	9H-Fluoren-2-yl	436.09
89	3-CF ₃	4-Acetamido	405.08

90	3-CF ₃	4-Carboxymethoxyl	422.05
91	4-OH	H	296.06
92	4-OH	4-Methoxy	326.07
93	4-OH	2-hydroxyl	312.06
94	4-OH	4-Dimethylamino	339.10
95	4-OH	4-Formyl	324.06
96	4-OH	4-Phenyl	372.09
97	4-OH	4-Naphthalen-2-yl	346.08
98	4-OH	4-Carboxyl	340.05
99	4-OH	2,4,5-Trimethoxyl	386.09
100	4-OH	9H-Fluoren-2-yl	384.09
101	4-OH	4-Methylthio	342.05
102	4-OH	4-Acetamido	353.08
103	4-OH	4-Carboxymethoxyl	370.06
104	4-Phenoxyl	H	372.09
105	4-Phenoxyl	Furan-2-yl	362.07
106	4-Phenoxyl	3-Nitro	417.08
107	4-Phenoxyl	4-Methoxy	402.10
108	4-Phenoxyl	2-hydroxyl	388.09
109	4-Phenoxyl	4-Dimethylamino	415.14
110	4-Phenoxyl	2-Cl	406.05
111	4-Phenoxyl	4-Formyl	400.09
112	4-Phenoxyl	4-Phenyl	448.12
113	4-Phenoxyl	4-Cyano	397.09
114	4-Phenoxyl	4-Naphthalen-2-yl	422.11
115	4-Phenoxyl	4-Carboxyl	416.08
116	4-Phenoxyl	2,4,5-Trimethoxyl	462.12
117	4-Phenoxyl	9H-Fluoren-2-yl	460.12
118	4-Phenoxyl	4-Methylthio	418.08
119	4-Phenoxyl	4-Acetamido	429.11
120	4-Phenoxyl	4-Carboxymethoxyl	446.09
121	4-Ethoxycarbonyl	H	352.09
122	4-Ethoxycarbonyl	Furan-2-yl	342.07
123	4-Ethoxycarbonyl	4-Cyano	377.08
124	4-Ethoxycarbonyl	4-Naphthalen-2-yl	402.10
125	4-Ethoxycarbonyl	4-Carboxyl	396.08
126	4-Ethoxycarbonyl	2,4,5-Trimethoxyl	442.12
127	4-Ethoxycarbonyl	4-Methylthio	398.08
128	4-Ethoxycarbonyl	4-Acetamido	409.11
129	4-Ethoxycarbonyl	4-Carboxymethoxyl	426.09
130	2-F	3-Methoxy-4-hydroxyl	344.06
131	2-F	4-Methoxy	328.07
132	2-F	2-hydroxyl	314.05
133	2-F	4-Dimethylamino	341.10
134	2-F	4-Phenyl	374.09
135	2-F	4-Naphthalen-2-yl	348.07
136	2-F	2,4,5-Trimethoxyl	388.09
137	2-F	4-Methylthio	344.05

138	2-F	4-hydroxyl	314.05
139	3-F	3-Methoxy-4-hydroxyl	344.06
140	3-F	4-Methoxy	328.07
141	3-F	2-hydroxyl	314.05
142	3-F	4-Dimethylamino	341.10
143	3-F	4-Phenyl	374.09
144	3-F	4-Naphthalen-2-yl	348.07
145	3-F	2,4,5-Trimethoxyl	388.09
146	3-F	4-Methylthio	344.05
147	3-F	4-Acetamido	355.08
148	3-F	4-hydroxyl	314.05
149	4-F	3-Methoxy-4-hydroxyl	344.06
150	4-F	4-Methoxy	328.07
151	4-F	2-hydroxyl	314.05
152	4-F	4-Dimethylamino	341.10
153	4-F	4-Phenyl	374.09
154	4-F	4-Naphthalen-2-yl	348.07
155	4-F	2,4,5-Trimethoxyl	388.09
156	4-F	4-Methylthio	344.05
157	4-F	4-Acetamido	355.08
158	4-F	4-hydroxyl	314.05
159	3-Me	3-Methoxy-4-hydroxyl	340.09
160	3-Me	4-Methoxy	324.09
161	3-Me	2-hydroxyl	310.08
162	3-Me	4-Dimethylamino	337.12
163	3-Me	4-Phenyl	370.11
164	3-Me	4-Naphthalen-2-yl	344.10
165	3-Me	2,4,5-Trimethoxyl	384.11
166	3-Me	4-Methylthio	340.07
167	3-Me	4-Acetamido	351.10
168	3-Me	4-hydroxyl	310.08
169	3-Cl	3-Methoxy-4-hydroxyl	360.03
170	3-Cl	2-hydroxyl	330.02
171	3-Cl	4-Dimethylamino	357.07
172	3-Cl	4-Phenyl	390.06
173	3-Cl	4-Naphthalen-2-yl	364.04
174	3-Cl	2,4,5-Trimethoxyl	404.06
175	3-Cl	4-Methylthio	360.02
176	3-Cl	4-Acetamido	371.05
177	3-MeO-4-OH	4-Methoxy	378.07
178	3-MeO-4-OH	2-hydroxyl	364.05
179	3-MeO-4-OH	4-Dimethylamino	391.10
180	3-MeO-4-OH	4-Phenyl	424.09
181	3-MeO-4-OH	4-Naphthalen-2-yl	398.07
182	3-MeO-4-OH	2,4,5-Trimethoxyl	438.09
183	3-MeO-4-OH	4-Methylthio	394.04
184	3-MeO-4-OH	4-Acetamido	405.08
185	3-MeO	2-hydroxyl	326.07

186	3-MeO	4-Dimethylamino	353.12
187	3-MeO	4-Phenyl	386.11
188	3-MeO	4-Naphthalen-2-yl	360.09
189	3-MeO	2,4,5-Trimethoxyl	400.11
190	3-MeO	4-Methylthio	356.07
191	3-MeO	4-Acetamido	367.10
192	3-MeO	4-hydroxyl	326.07
193	4-MeO	4-Methoxy	340.09
194	4-MeO	4-Dimethylamino	353.12
195	4-MeO	4-Phenyl	386.11
196	4-MeO	4-Naphthalen-2-yl	360.09
197	4-MeO	2,4,5-Trimethoxyl	400.11
198	4-MeO	4-Methylthio	356.07
199	4-MeO	4-Acetamido	367.10
200	3-OH	3-Methoxy-4-hydroxyl	342.07
201	3-OH	4-Phenyl	372.09
202	3-OH	4-Naphthalen-2-yl	346.08
203	3-OH	2,4,5-Trimethoxyl	386.09
204	3-OH	4-Acetamido	353.08
205	3-OH	4-hydroxyl	312.06
206	2-Me	4-hydroxyl	310.08
207	4-Me	4-hydroxyl	310.08
208	2-Cl	4-hydroxyl	330.02
209	4-Cl	4-hydroxyl	330.02
210	2-MeO	4-hydroxyl	326.07

Table S3. ¹H-NMR and high-resolution mass spectrometry of compounds.

Compound	¹H-NMR (400 MHz, DMSO)	HR-MS
48	δ 8.20(s, 1H), 7.82-7.87(m, 2H), 7.75(s, 1H), 7.25-7.60(m, 9H), 4.12(s, 2H); ESI-MS: m/z 403.0328(M+1)	m/z 403.0328(M+1)
49	δ 8.30(s, 1H), 7.72(s, 1H), 7.25-7.60(m, 8H), 2.55(s, 3H)	m/z 361.0258(M+1)
53	δ 8.10(s, 1H), 7.85-7.90(m, 2H), 7.40-7.60(m, 6H), 7.10(d, J = 16.2, 2H), 4.15(s, 2H)	m/z 403.8325(M+1)
69	δ 8.10(m, 3H), 7.80(s, 1H), 7.75(t, 1H), 7.20-7.40(m, 5H)	m/z 360.0201(M+1)
93	δ 8.15(s, 2H), 7.60(d, J = 7.8, 1H), 7.16(m, 3H), 6.7-6.9(m, 4H), 5.35(s, 2H)	m/z 311.0494(M-1)
139	δ 8.00(s, 1H), 7.72(s, 1H), 7.43(m, 1H), 6.90-7.16(m, 5H), 6.75(d, J = 7.8, 1H), 5.30(s, 1H), 3.8(s, 3H)	m/z 345.0707(M+1)
140	δ 8.20(s, 1H), 7.75(s, 1H), 7.63(d, J = 16.2, 2H), 7.43(m, 1H), 6.75-7.24(m, 5H), 3.8(s, 3H)	m/z 329.0743(M+1)
142	δ 8.35(s, 1H), 7.80(s, 1H), 7.15-7.45(m, 5H), 6.74(m, 3H), 3.06(s, 6H)	m/z 342.1063(M+1)
156	δ 8.30(s, 1H), 7.70(s, 1H), 7.24-7.45(m, 8H), 2.53(s, 3H)	m/z 345.0521(M+1)
165	δ 8.60(s, 1H), 8.00(s, 1H), 7.23-7.33(m, 2H), 6.80(m, 4H), 3.85(s, 9H), 2.34(s, 3H)	m/z 385.1215(M+1)

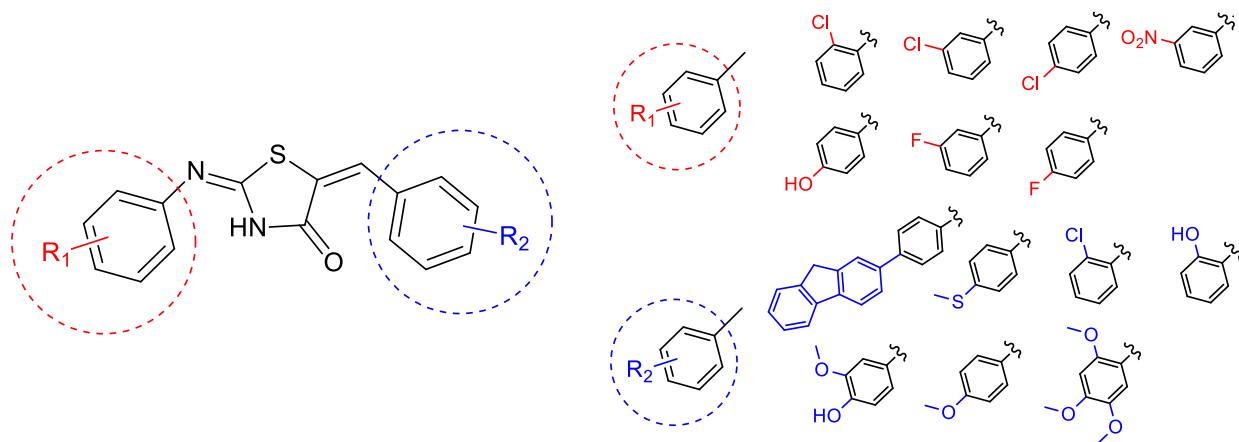


Figure S1

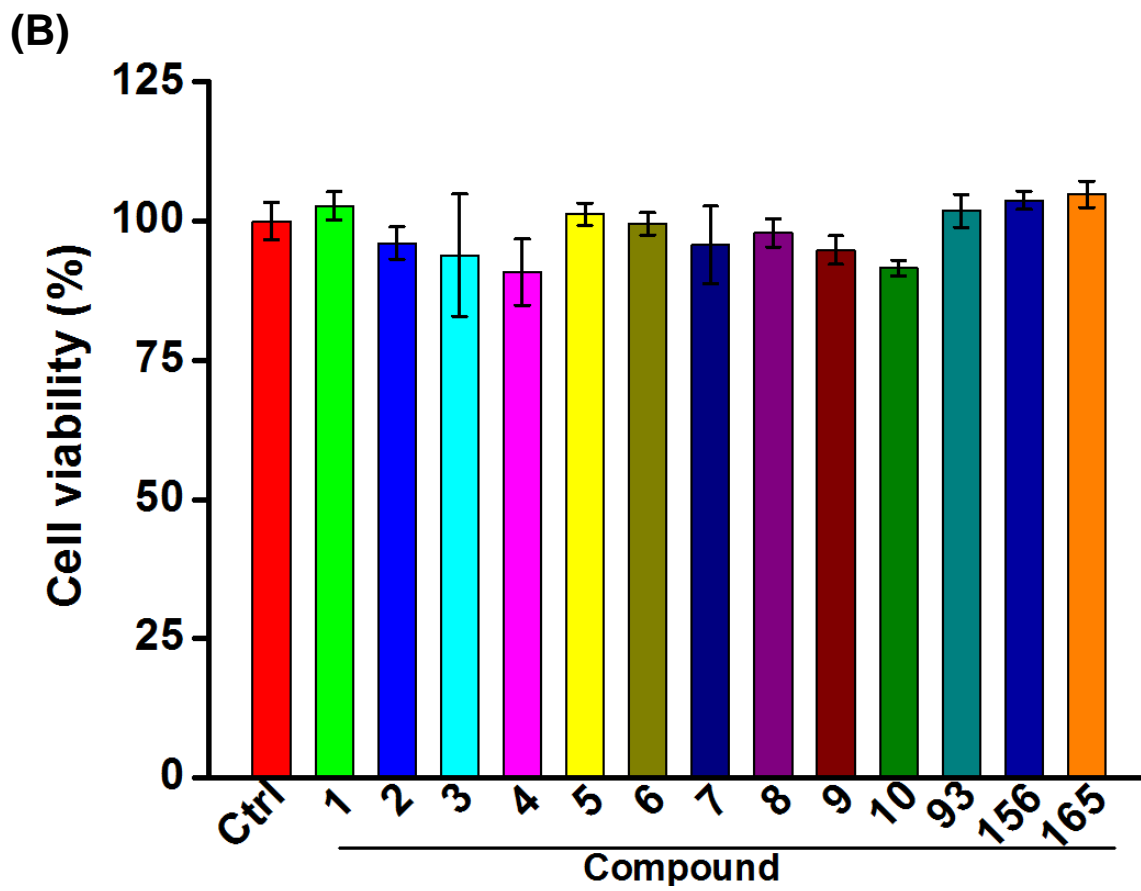
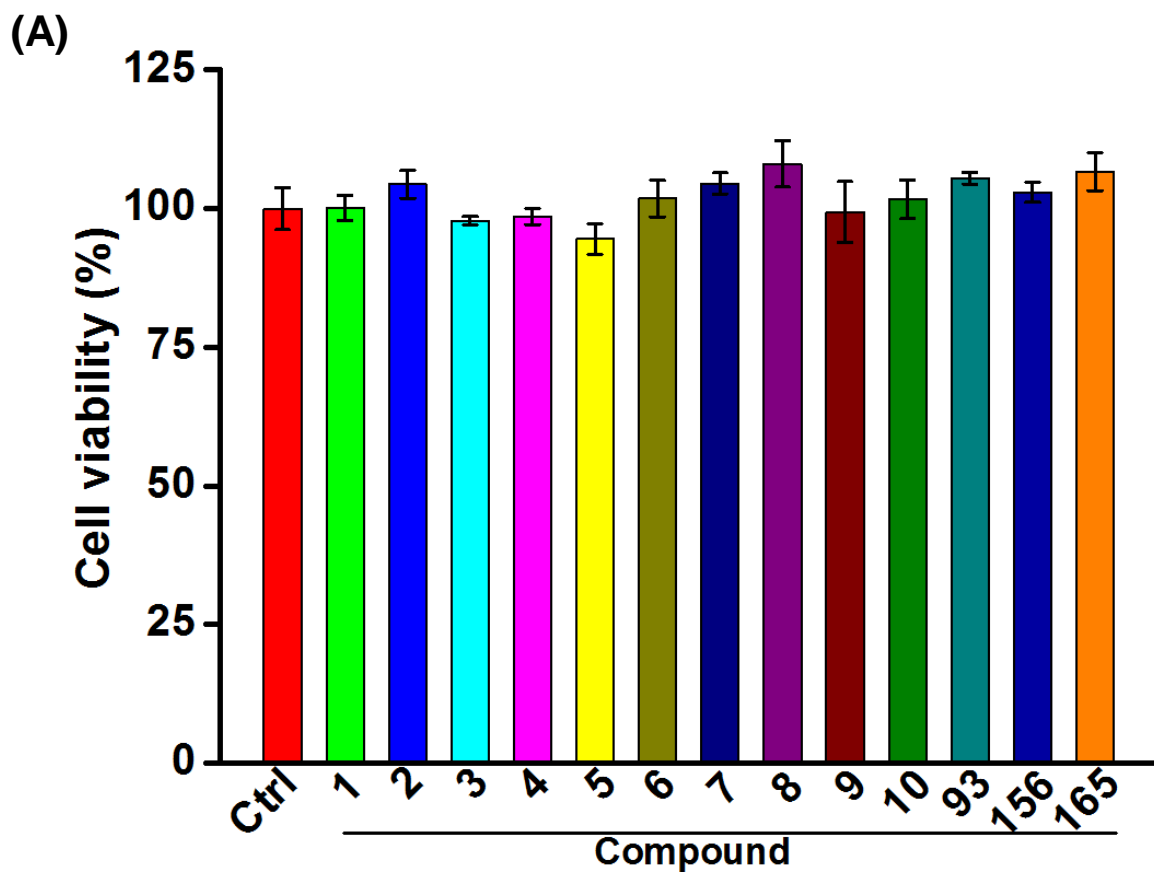


Figure S2

(A)

Compound No.	6 h	24 h
	Liver hepcidin mRNA	Liver hepcidin mRNA
Ctrl	1.00 ± 0.35	1.00 ± 0.16
48	1.26 ± 0.20	1.19 ± 0.17
49	1.01 ± 0.59	$1.67 \pm 0.11^*$
53	1.45 ± 0.69	1.10 ± 0.18
69	1.10 ± 0.43	1.28 ± 0.17
93	$1.80 \pm 0.30^*$	$2.03 \pm 0.38^*$
139	$1.97 \pm 0.10^\#$	1.38 ± 0.21
140	1.04 ± 0.17	$1.64 \pm 0.20^*$
142	1.16 ± 0.31	1.59 ± 0.66
156	$1.56 \pm 0.16^*$	$1.68 \pm 0.21^*$
165	1.36 ± 0.14	$2.04 \pm 0.37^*$

(B)

Compound No.	Chemical Structure	Administration time			
		6 h		24 h	
		Serum hepcidin (ng/mL)	Serum iron ($\mu\text{g/dL}$)	Serum hepcidin (ng/mL)	Serum iron ($\mu\text{g/dL}$)
Ctrl	—	10.79 ± 0.30	522.01 ± 16.65	11.21 ± 0.24	524.56 ± 8.87
48		12.63 ± 0.92	566.18 ± 98.11	8.19 ± 1.22	530.46 ± 98.31
49		9.39 ± 0.96	551.38 ± 33.81	9.19 ± 0.33	591.85 ± 32.03
53		13.02 ± 0.96	518.07 ± 33.08	12.32 ± 0.92	578.76 ± 66.44
69		$14.88 \pm 1.19^*$	494.42 ± 91.75	14.13 ± 1.05	422.78 ± 94.70
93		$14.35 \pm 0.52^*$	$446.59 \pm 28.29^*$	$15.52 \pm 1.34^*$	$412.82 \pm 12.31^\#$
139		$16.29 \pm 0.70^*$	$475.84 \pm 64.04^*$	8.63 ± 2.43	513.83 ± 63.44
140		12.74 ± 4.17	528.33 ± 71.62	11.35 ± 2.14	588.61 ± 63.43
142		12.72 ± 0.70	537.23 ± 105.16	8.57 ± 1.35	499.12 ± 62.98
156		$14.64 \pm 0.82^\#$	$474.13 \pm 32.94^\#$	$17.71 \pm 1.01^*$	$425.56 \pm 13.97^\#$
165		$15.78 \pm 0.38^\#$	$463.60 \pm 20.38^*$	$16.52 \pm 0.64^*$	$441.54 \pm 14.69^\#$

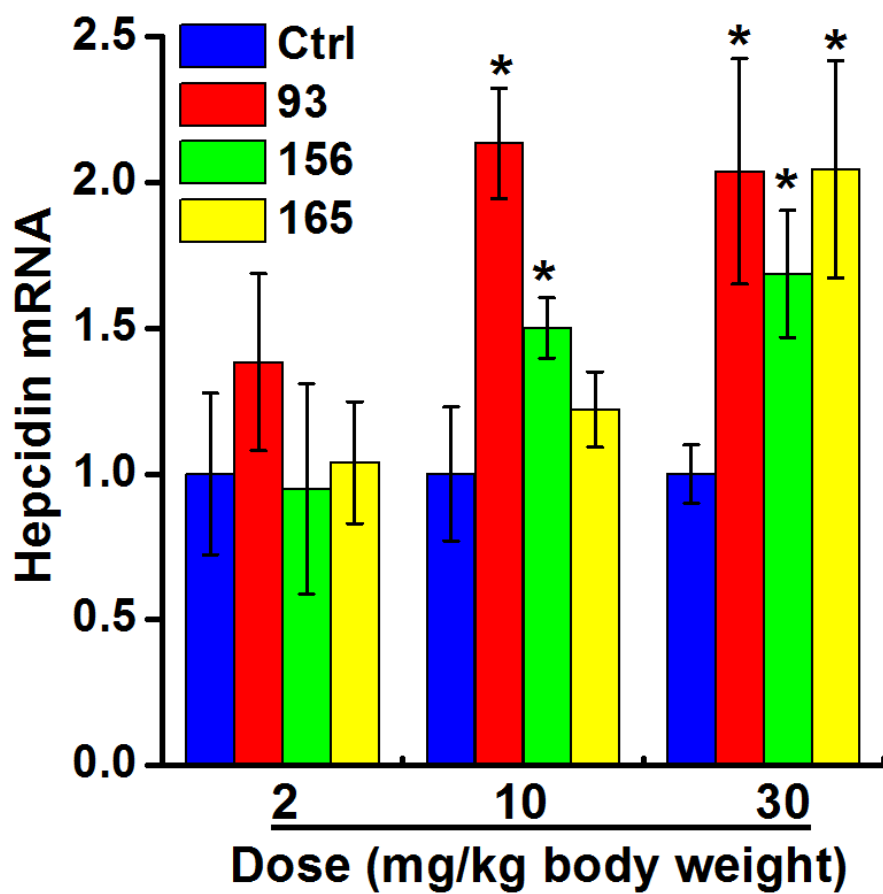


Figure S4

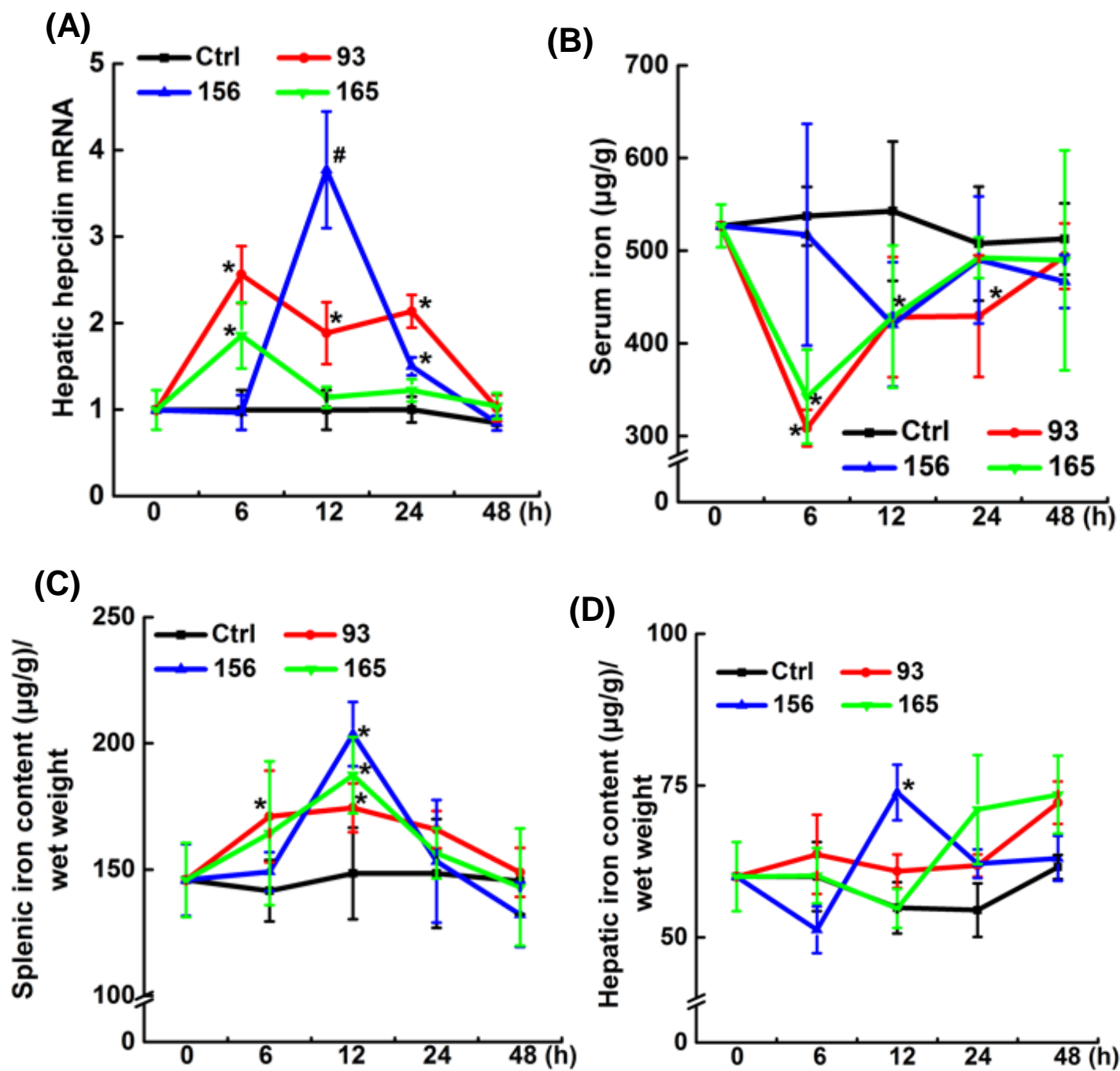


Figure S5

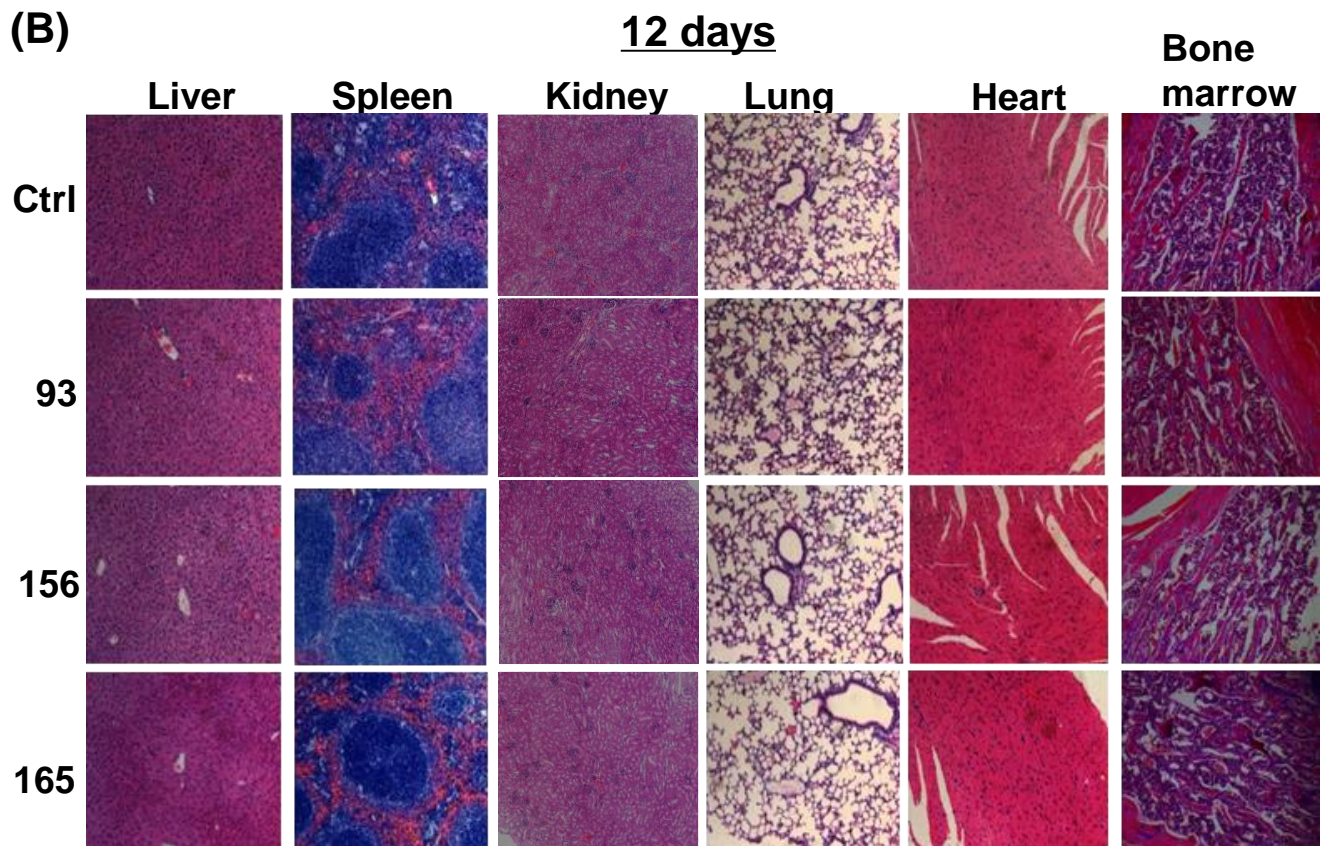
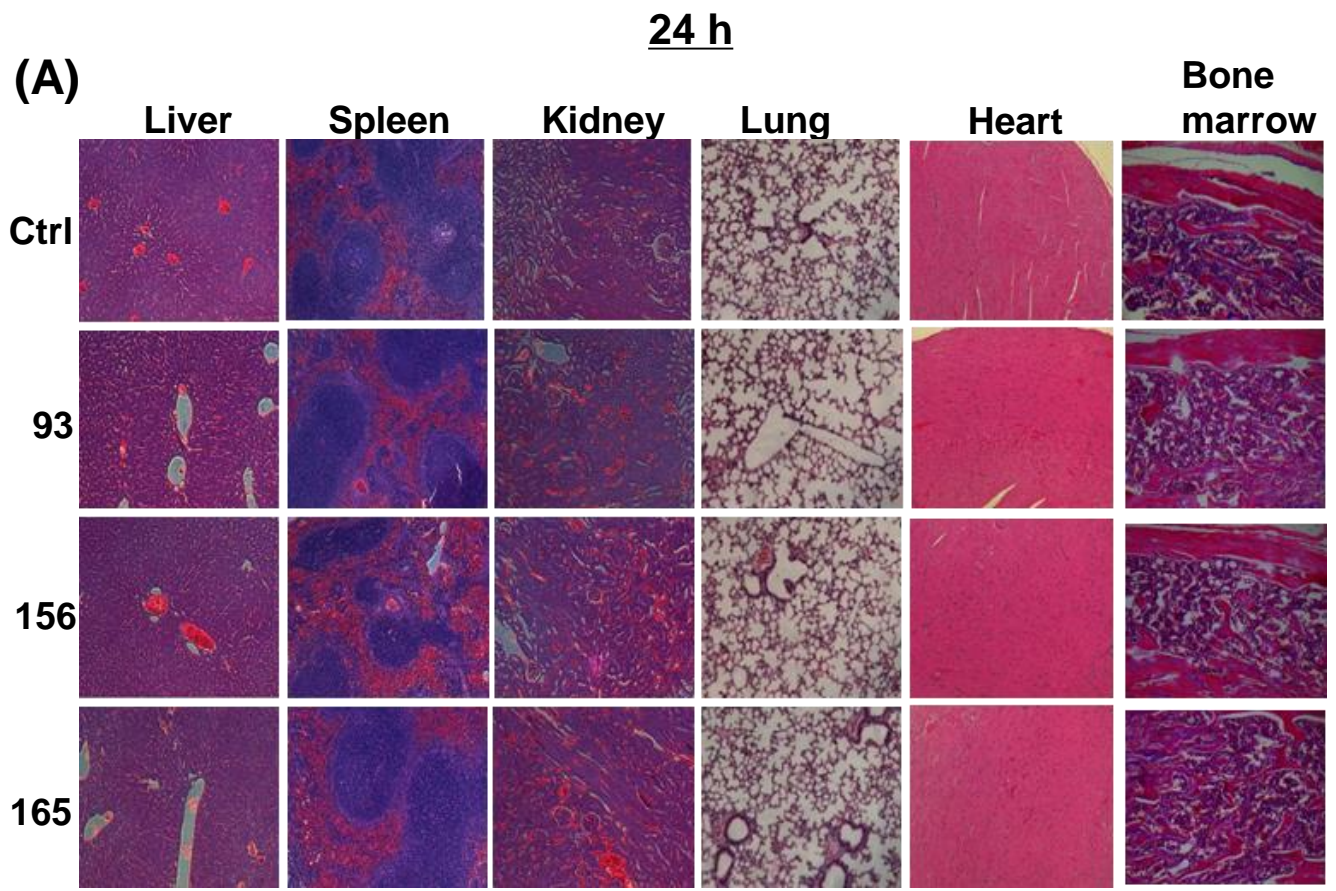


Figure S6

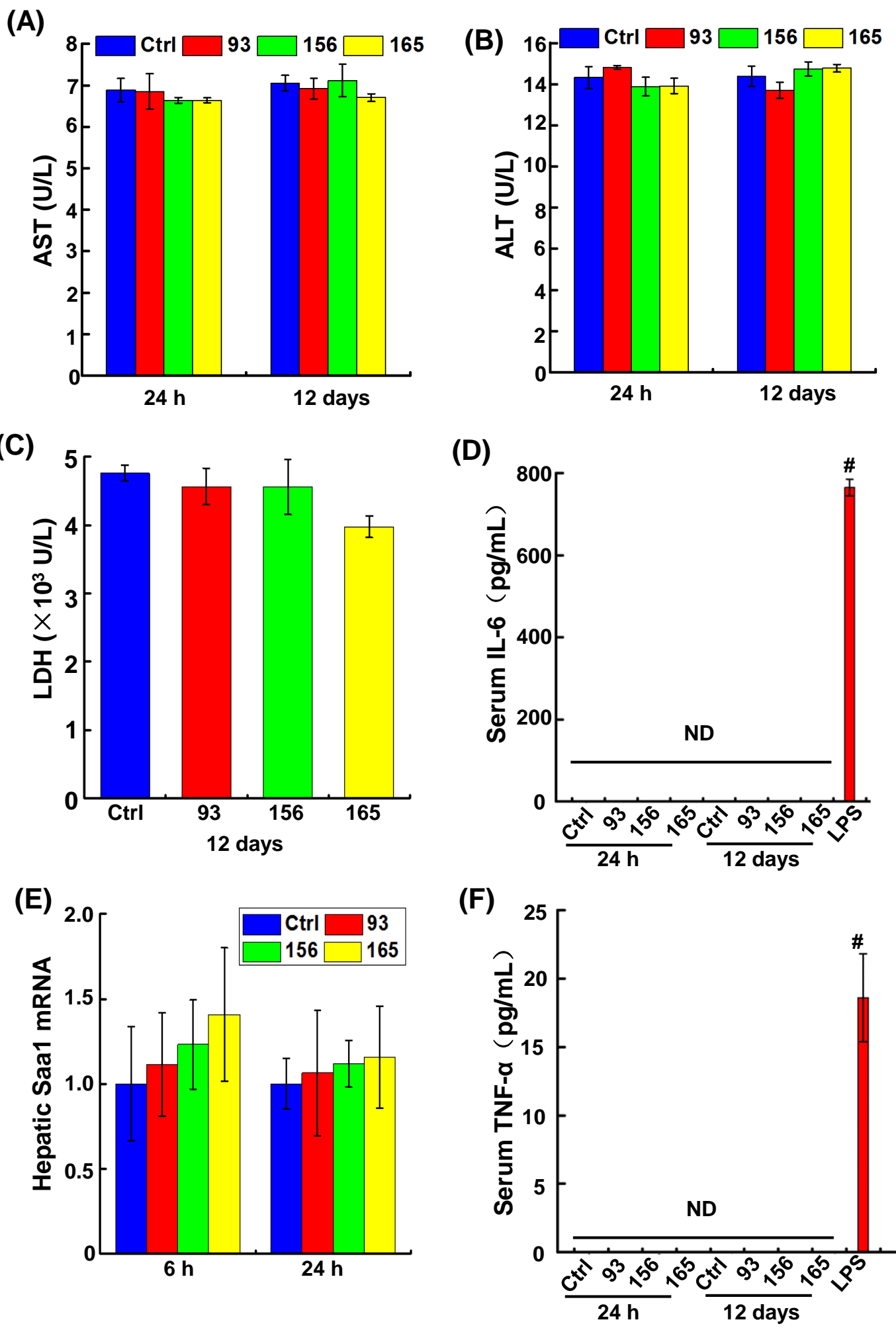


Figure S7

(A)

	Ctrl	93	156	165
RBC ($\times 10^{12}/L$)	9.2\pm0.56	8.7\pm0.73	9.1\pm0.28	8.8\pm0.66
HGB (g/L)	134.0\pm8.17	124.3\pm10.20	133.3\pm3.68	124.6\pm9.74
MCV (fL)	44.3\pm0.83	44.0\pm0.71	44.4\pm0.78	44.9\pm0.23
MCH (pg)	14.3\pm0.12	14.2\pm0.12	14.6\pm0.23	14.5\pm0.26
MCHC (g/L)	324\pm3.39	325\pm2.16	329\pm2.05	322\pm4.18
HCT%	47.82\pm2.06	40.71\pm4.10	42.50\pm4.06	46.47\pm1.54
RDW%	13.46\pm0.28	13.30\pm0.10	13.47\pm0.24	13.52\pm0.12
WBC($\times 10^9/L$)	2.14\pm0.41	2.06\pm0.23	2.20\pm0.44	2.52\pm0.19
LY%	83.60\pm5.73	77.20\pm5.84	84.80\pm8.52	71.58\pm12.57

(B)

	Ctrl	93	156	165
RBC ($\times 10^{12}/L$)	9.1\pm0.44	8.6\pm0.43	8.63\pm0.27	8.95\pm0.61
HGB (g/L)	148.4\pm6.62	144.0\pm2.12	144.5\pm4.77	149.6\pm4.18
MCV (fL)	46.28\pm0.29	46.53\pm0.27	47.08\pm0.33	47.24\pm0.37
MCH (pg)	15.92\pm0.31	16.08\pm0.34	15.94\pm0.14	16.04\pm0.24
MCHC (g/L)	344.0\pm7.13	346.0\pm5.94	338.6\pm4.76	339.0\pm4.81
HCT%	43.18\pm2.57	43.02\pm2.71	42.75\pm5.52	43.43\pm1.51
RDW%	13.62\pm0.25	13.78\pm.24	13.58\pm0.20	14.06\pm0.28
WBC($\times 10^9/L$)	2.53\pm0.09	2.70\pm0.42	2.70\pm0.25	2.90\pm0.18
LY%	80.97\pm0.96	78.40\pm3.78	75.27\pm4.21	77.10\pm5.54

Figure S8

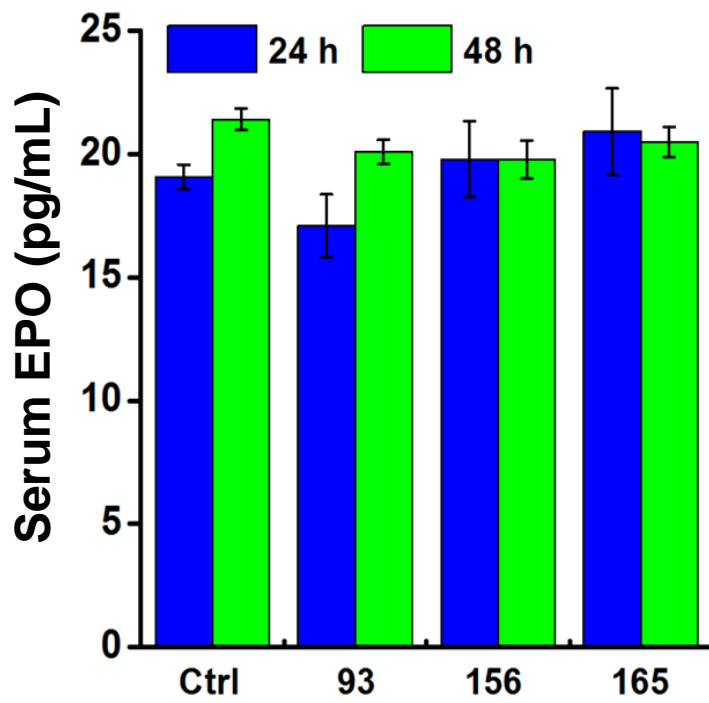
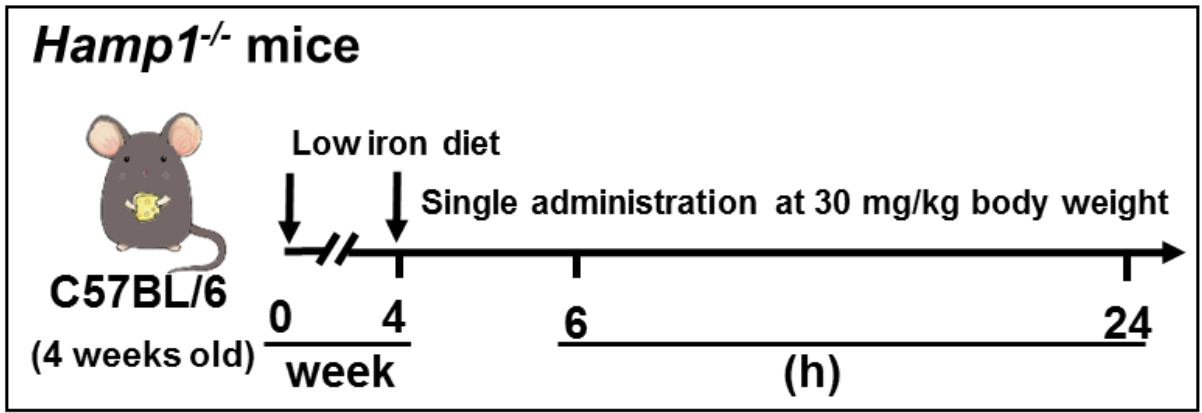
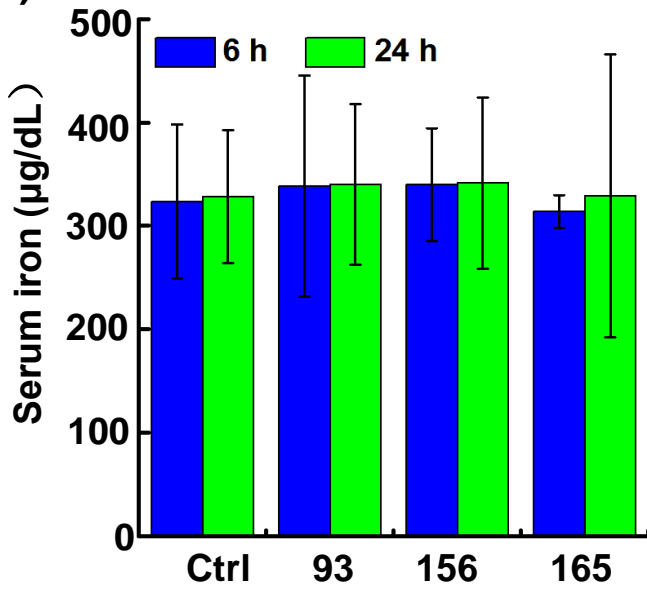


Figure S9

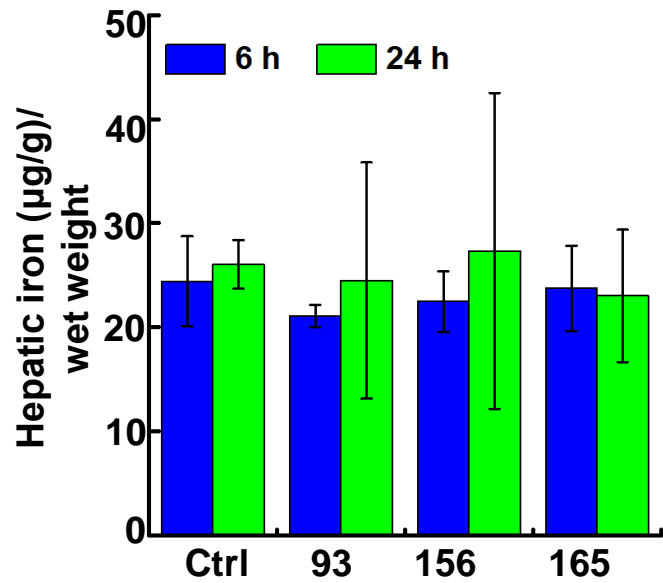
(A)



(B)



(C)



(D)

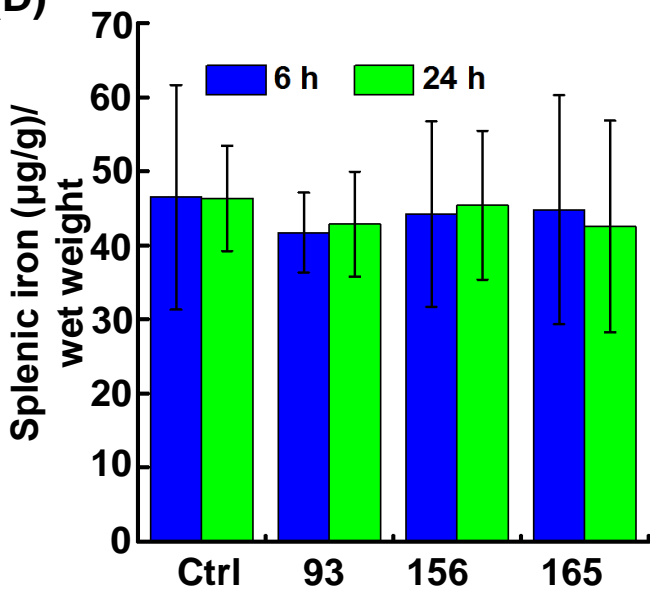


Figure S10

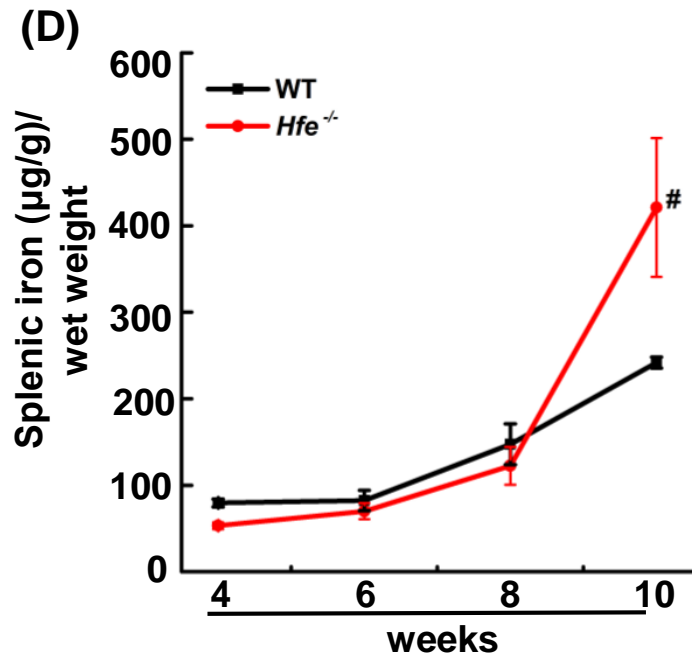
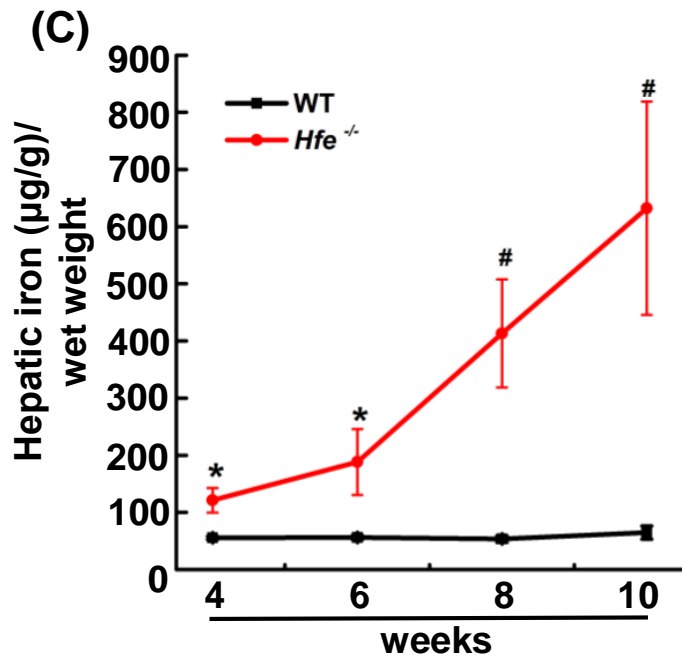
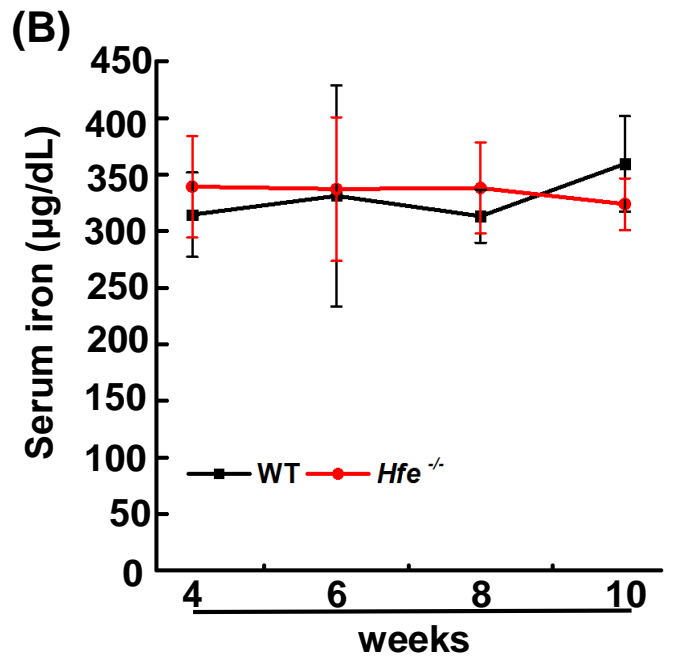
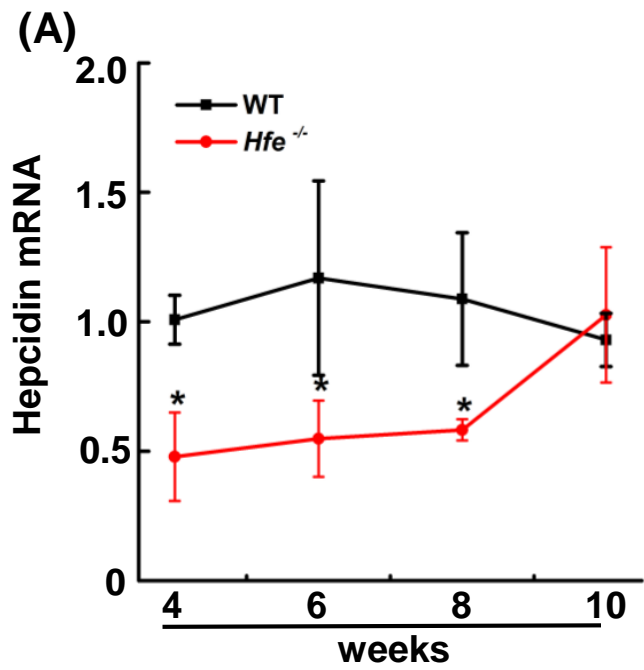


Figure S11

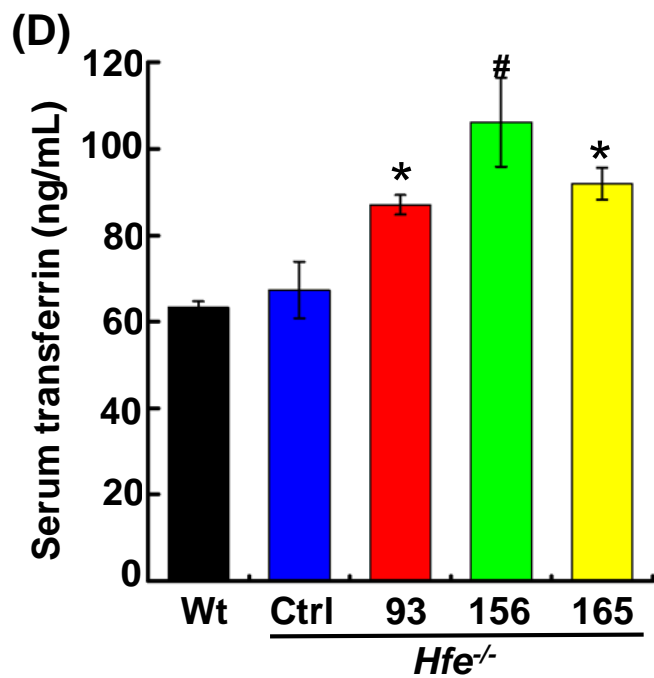
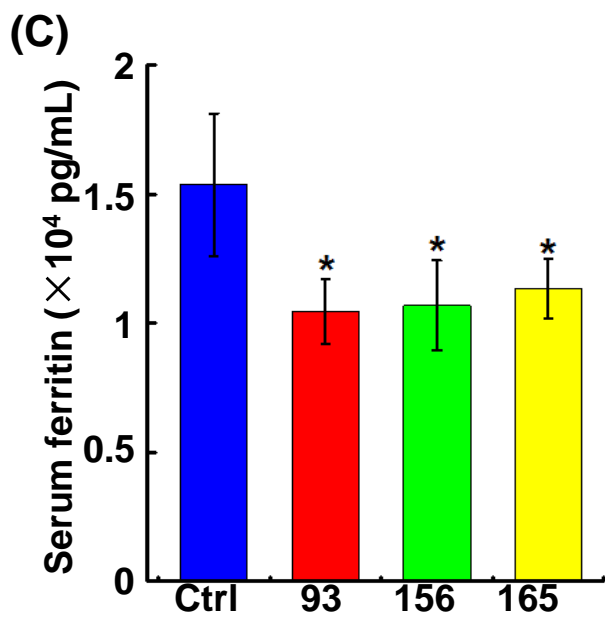
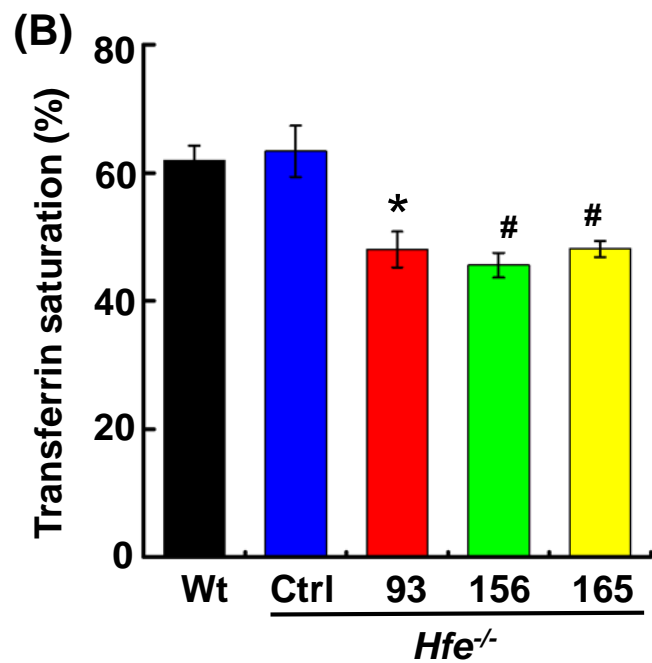
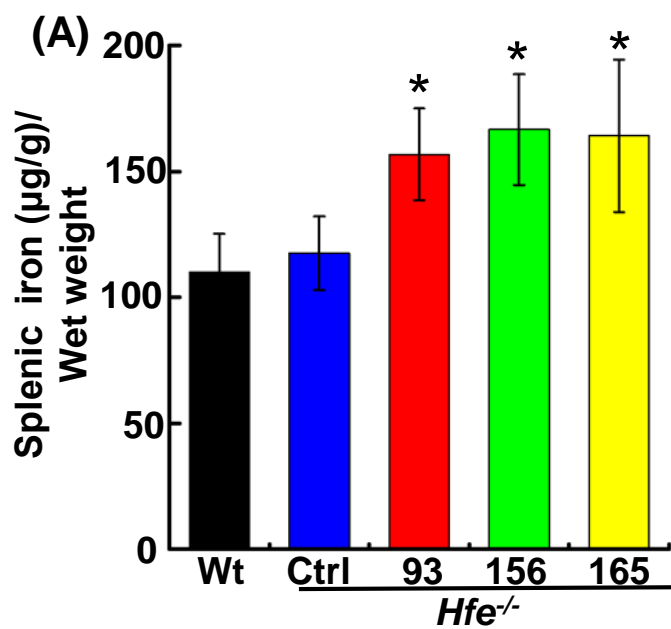


Figure S12

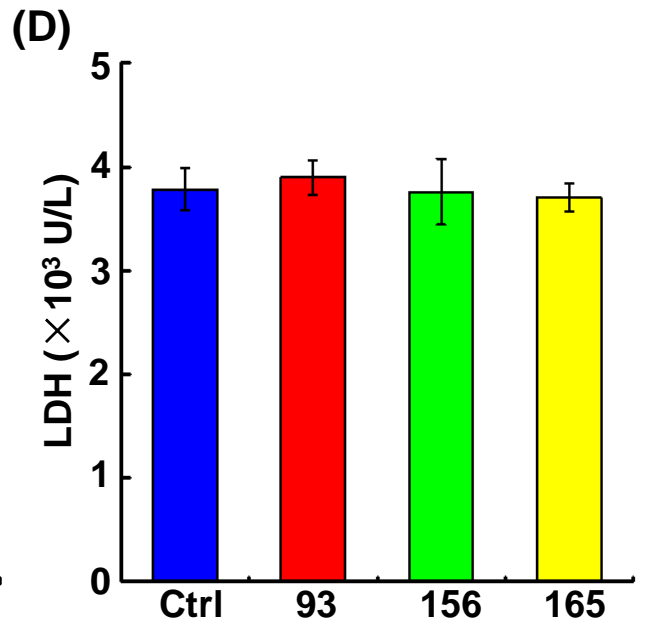
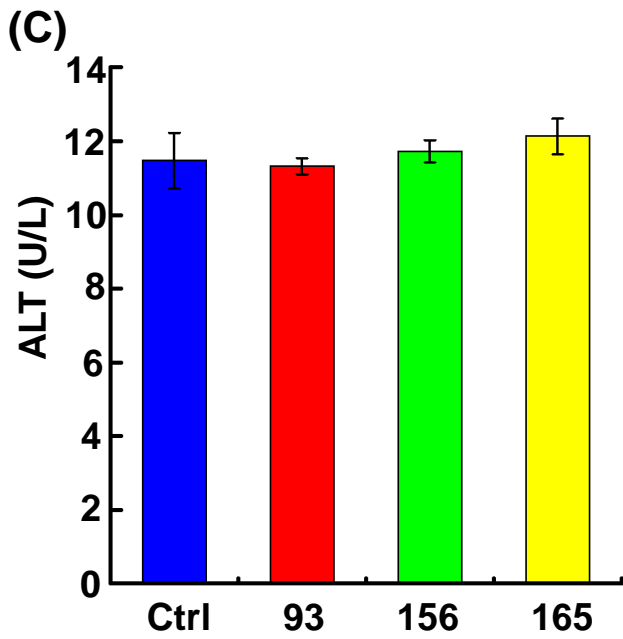
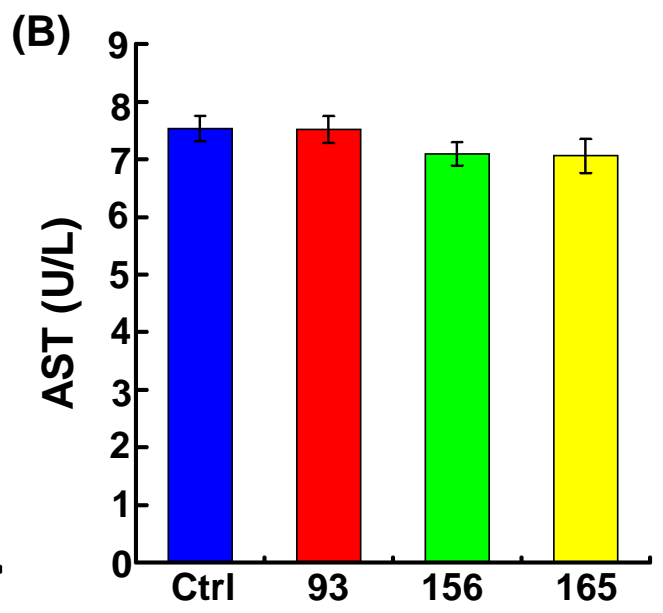
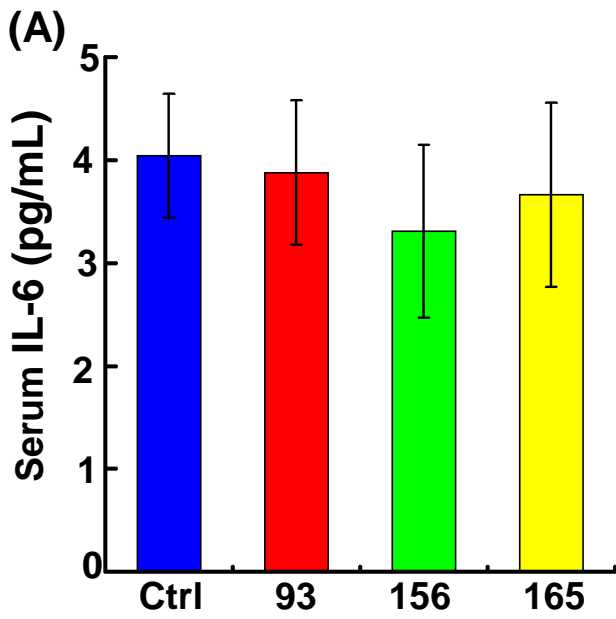
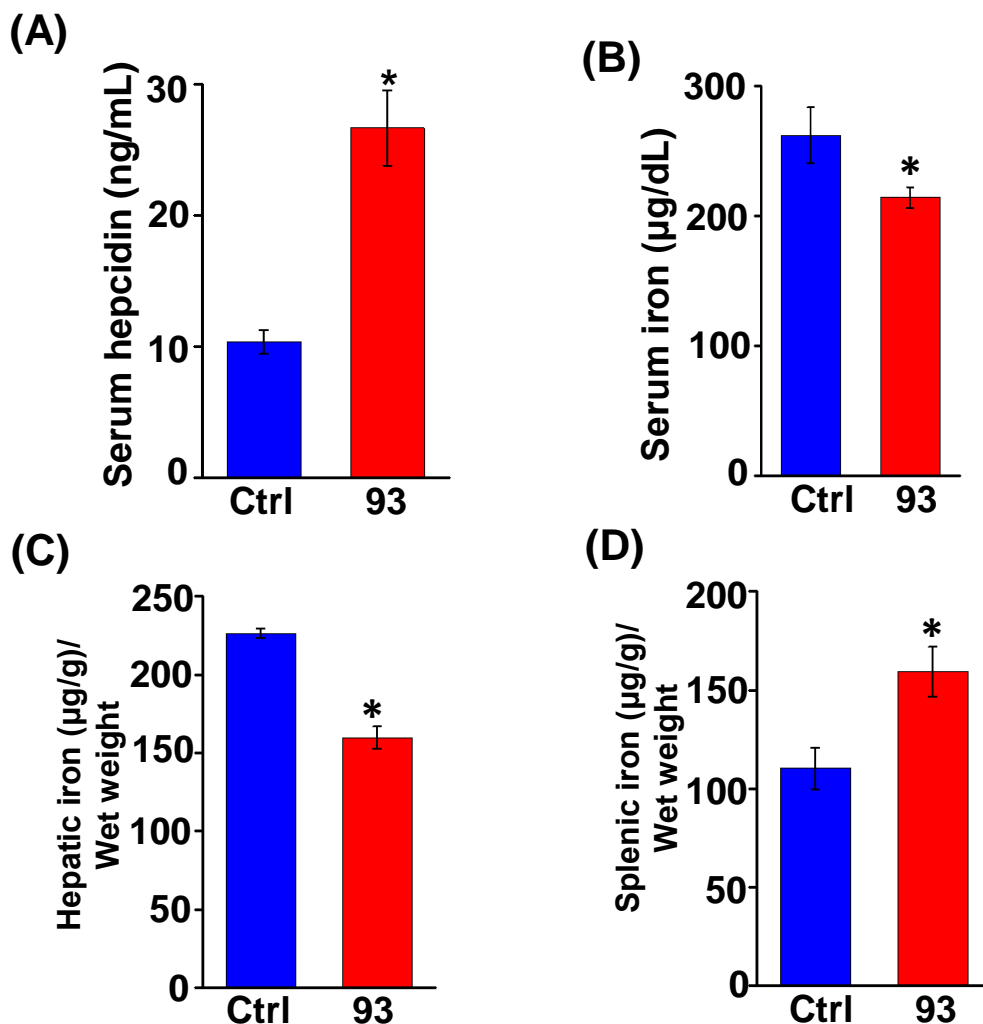
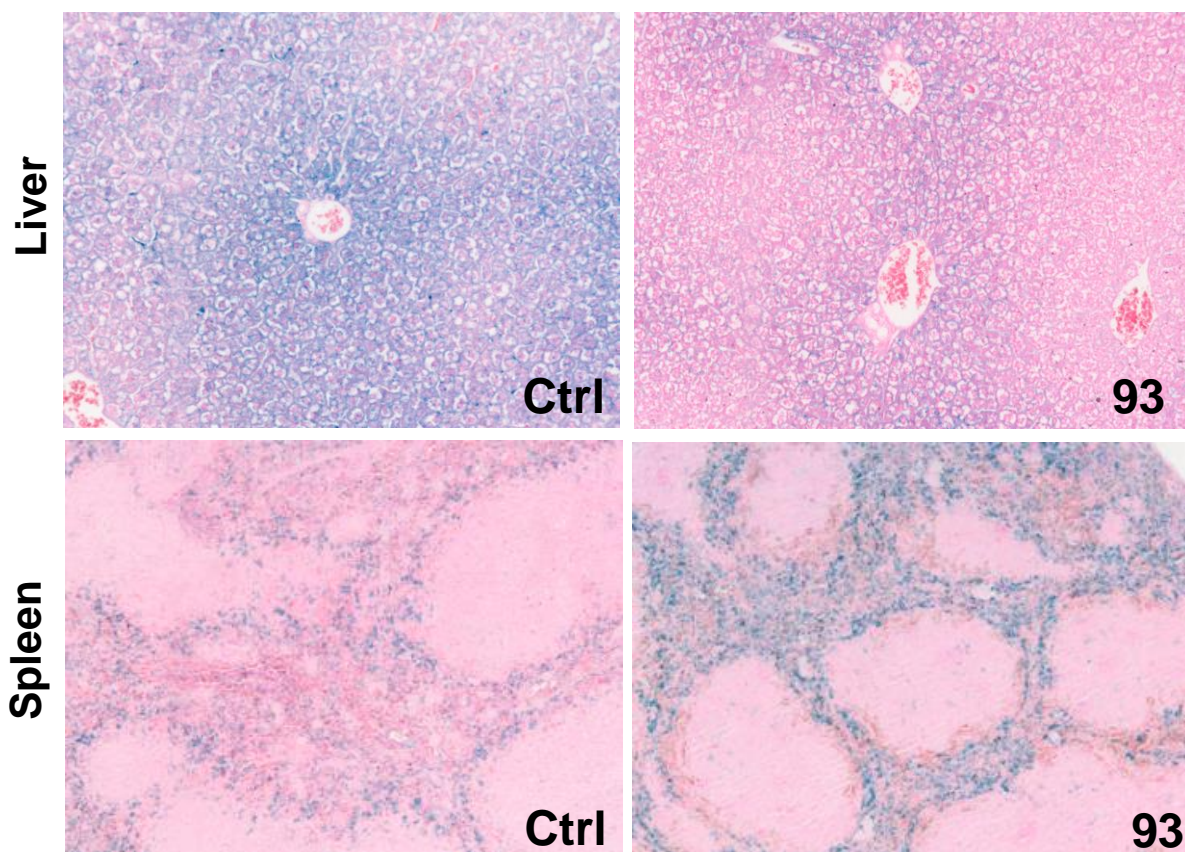


Figure S13



(E)



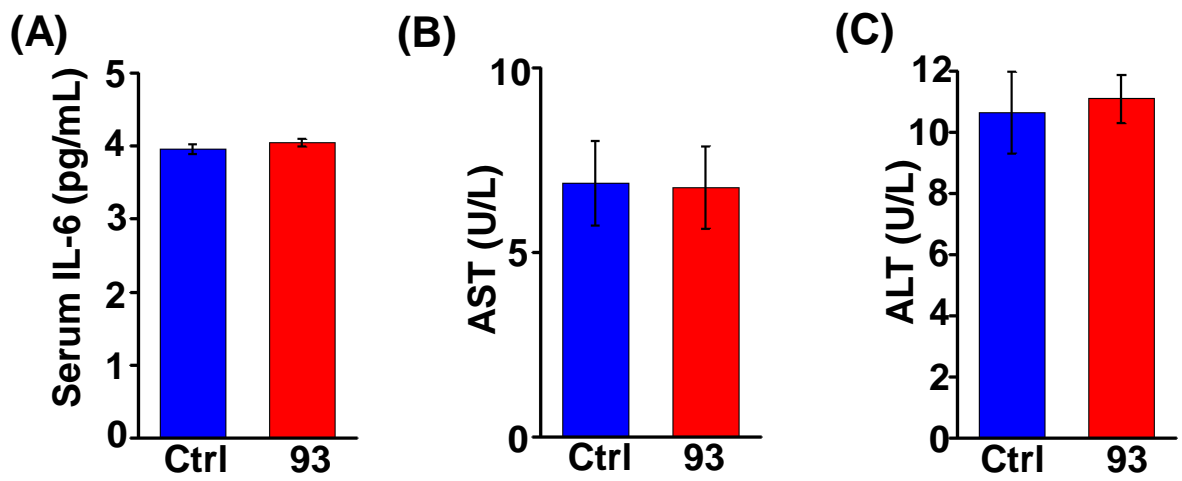
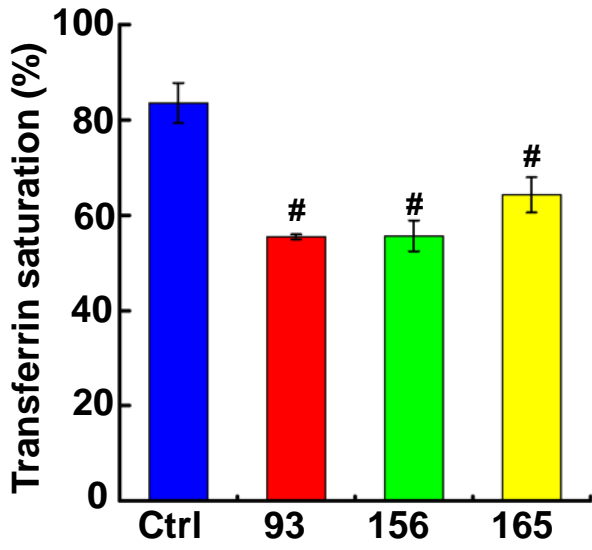


Figure S15

(A)



(B)

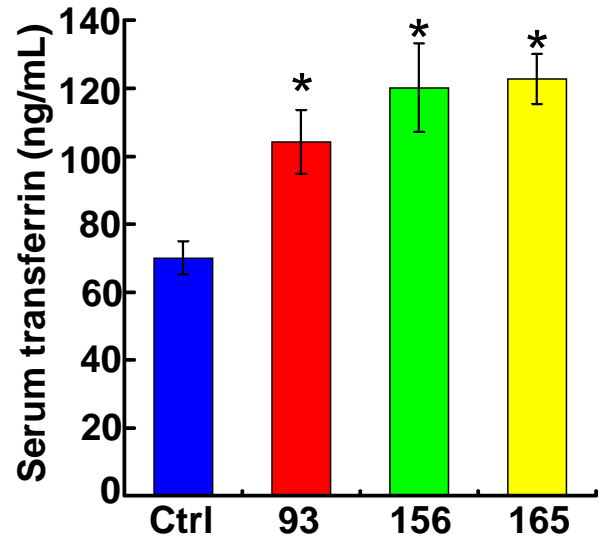


Figure S16

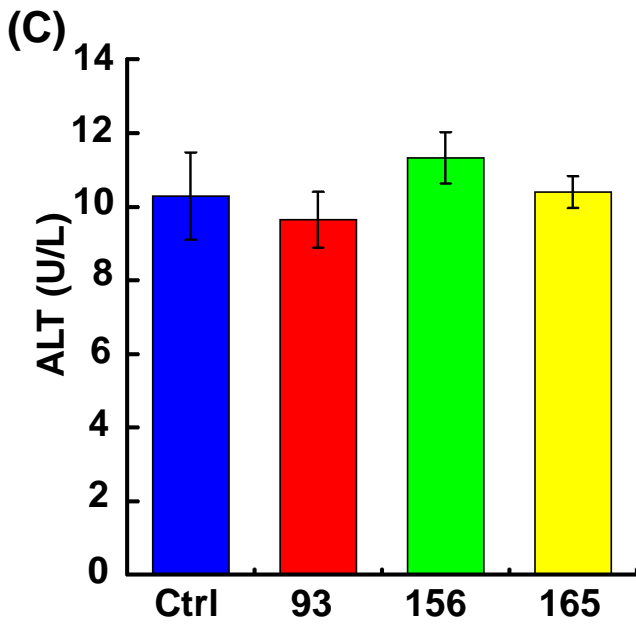
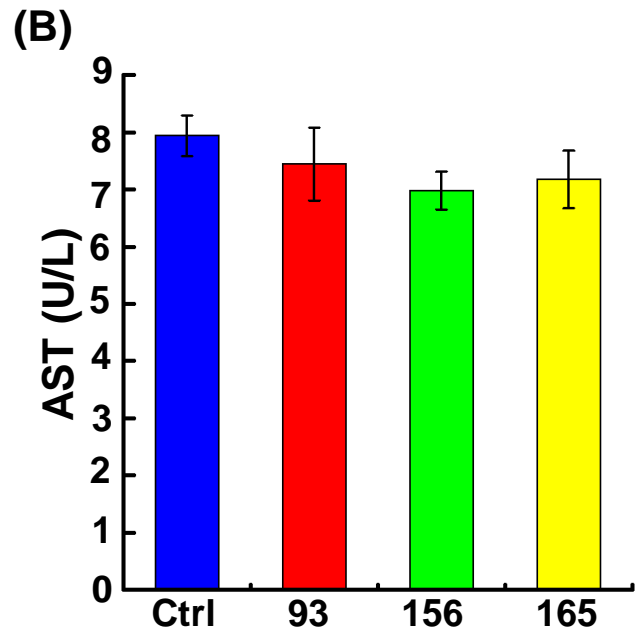
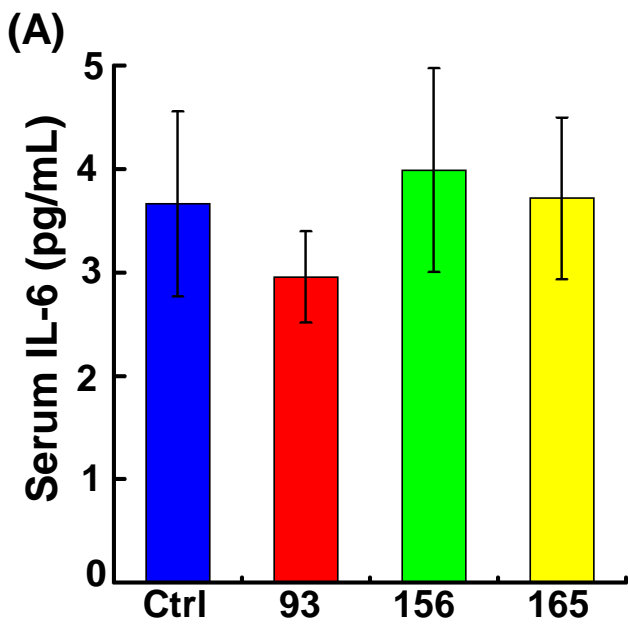


Figure S17

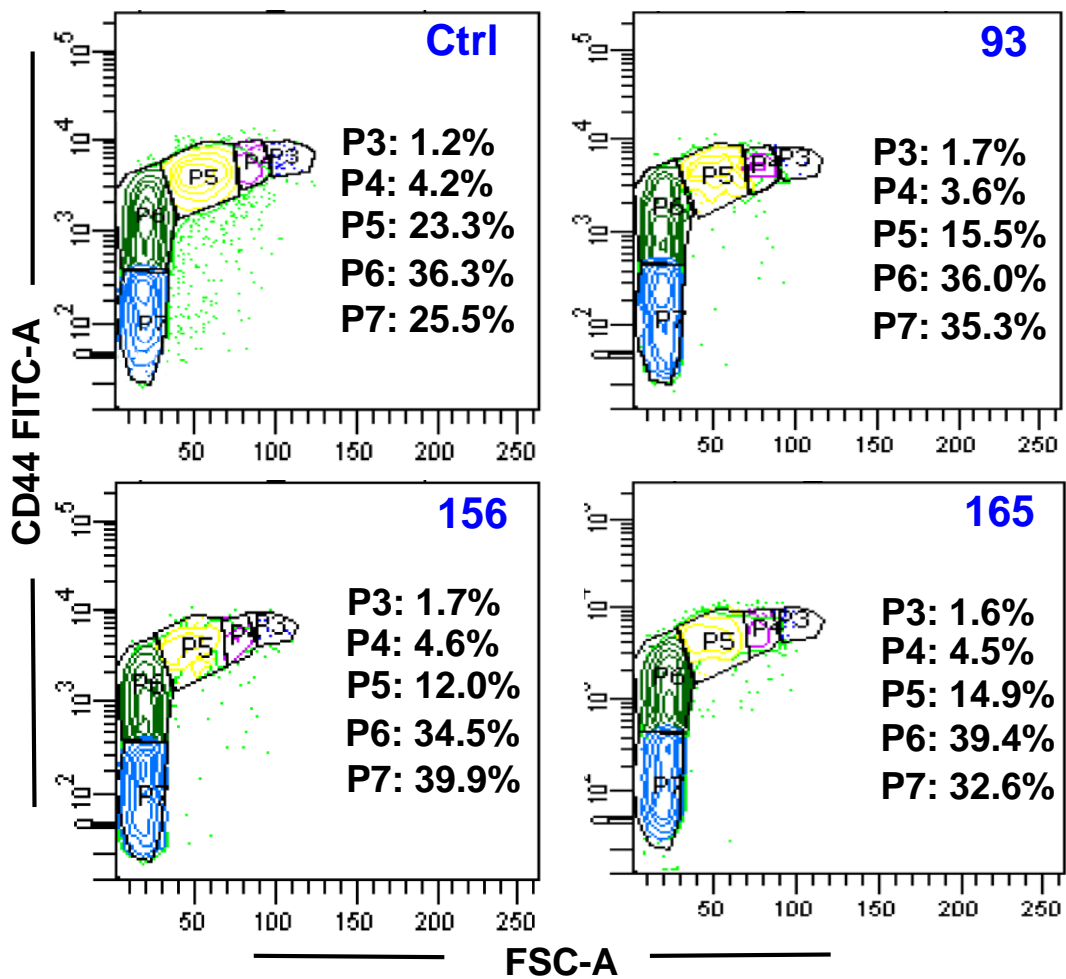


Figure S18

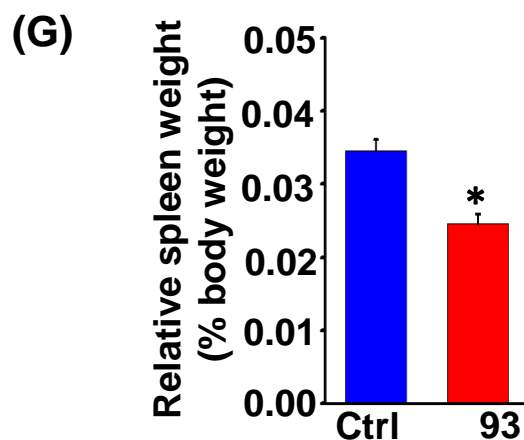
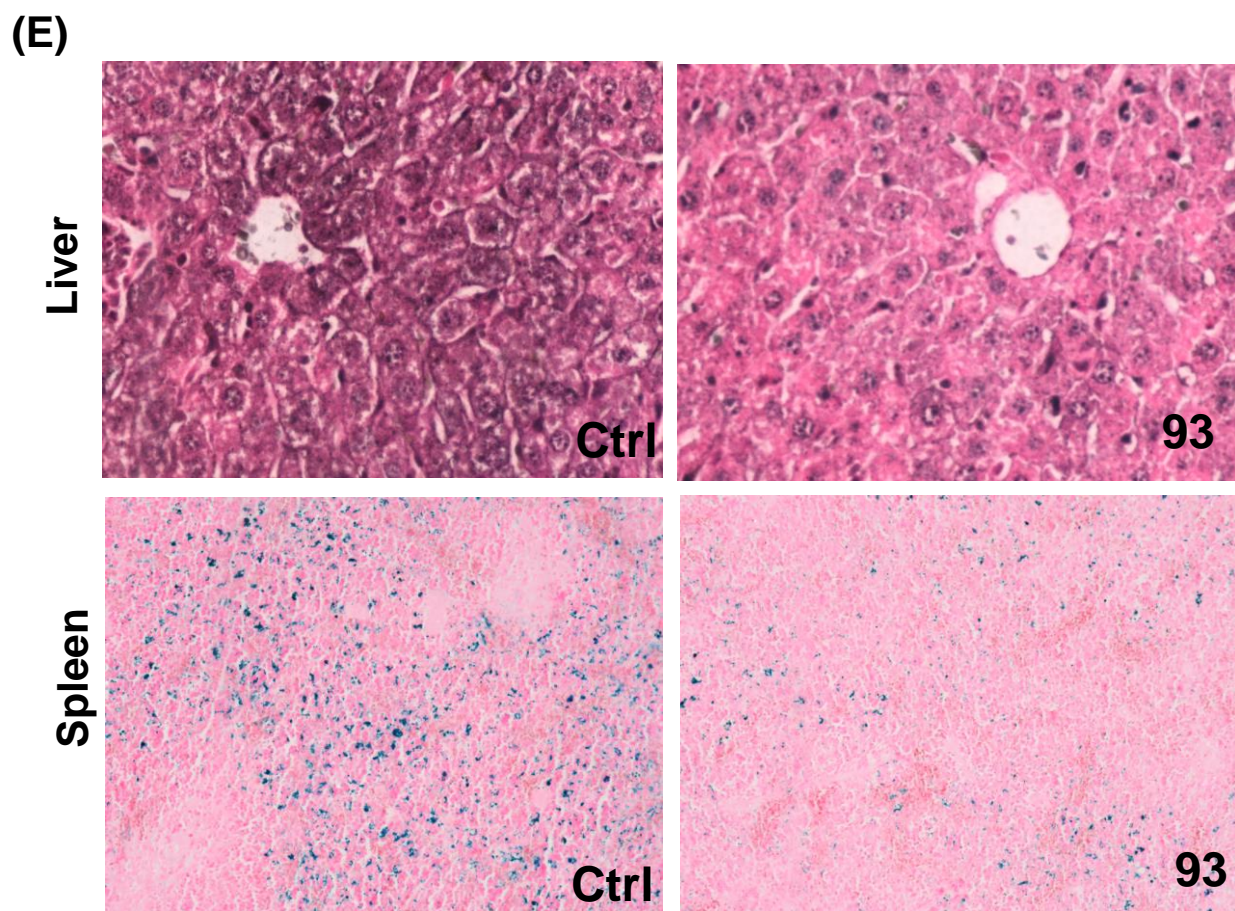
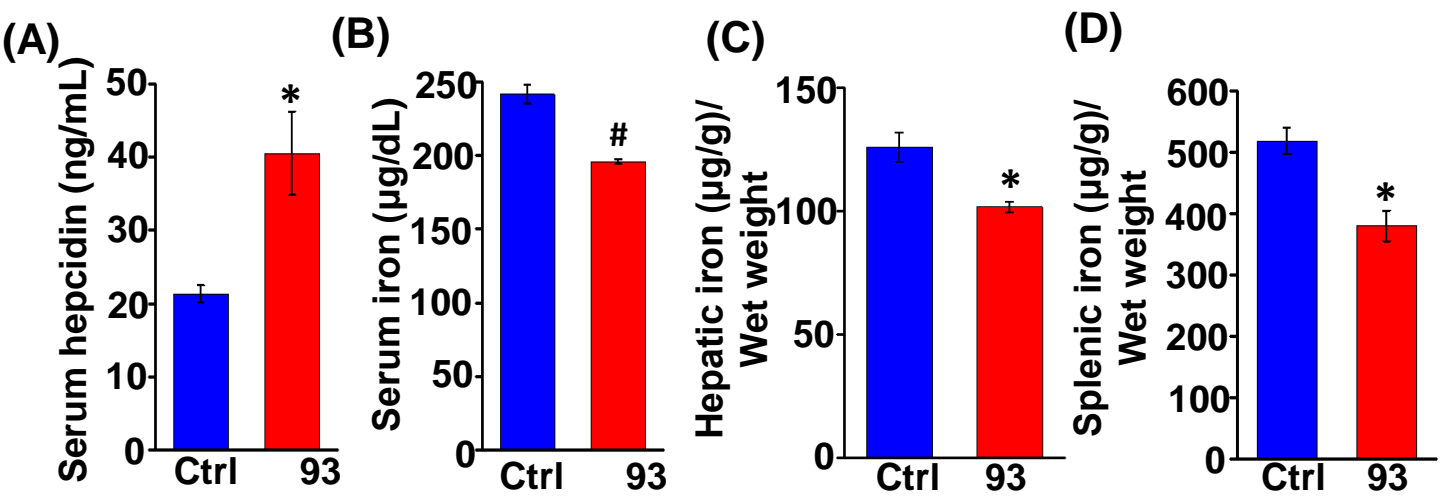
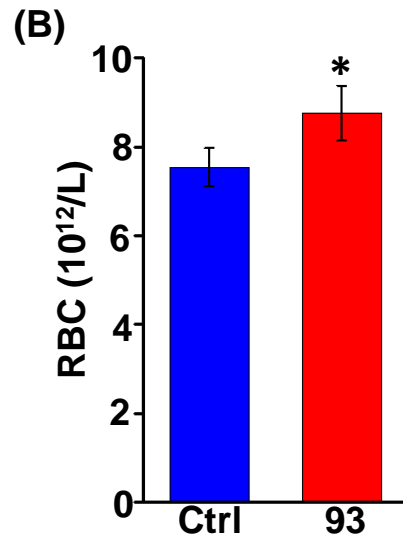
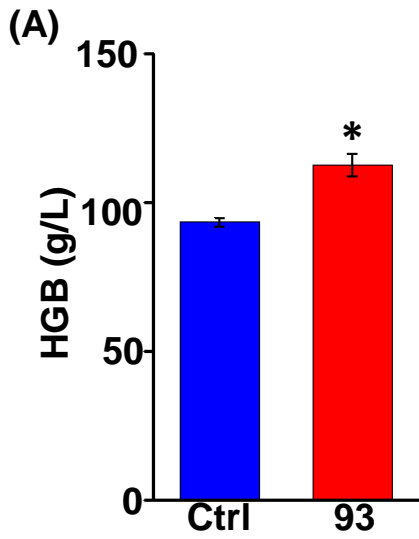
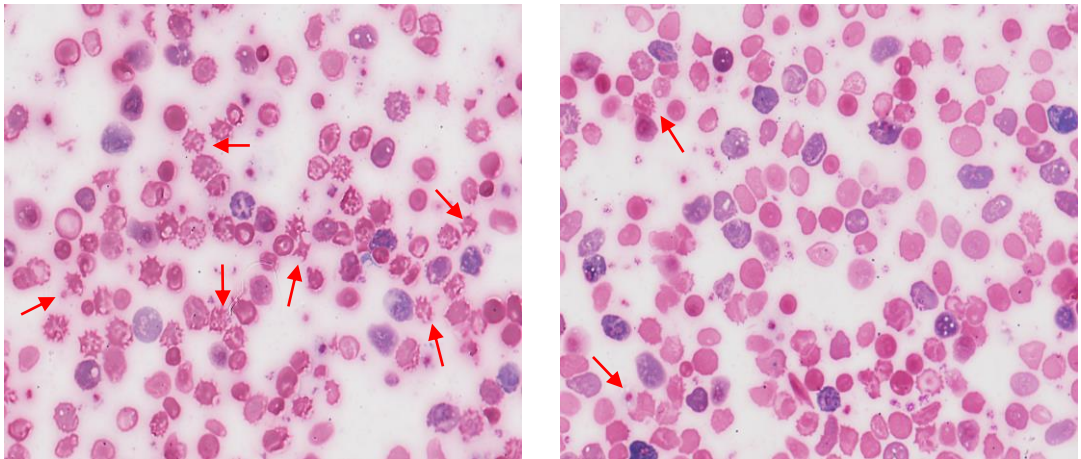


Figure S19



(C)



(D)

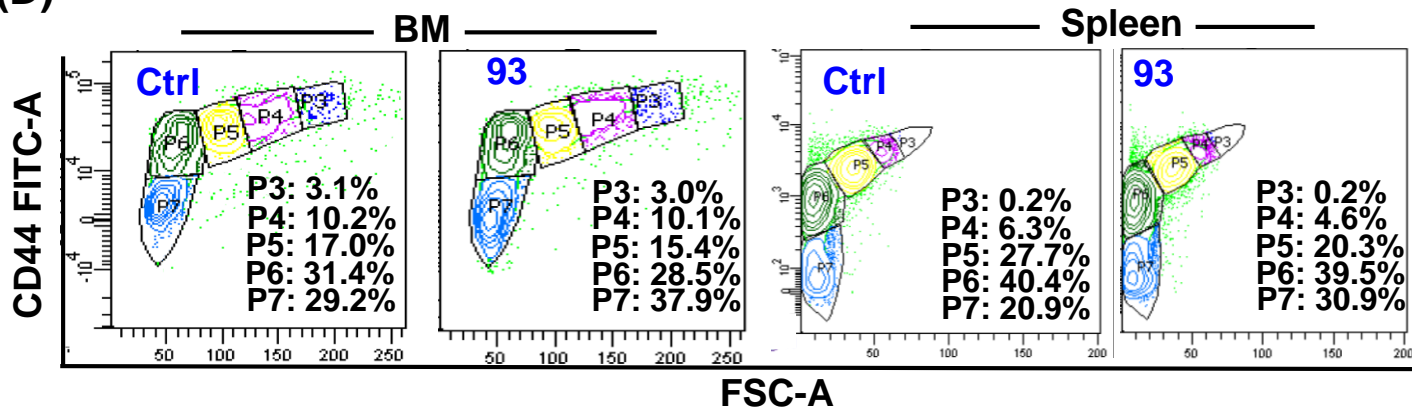
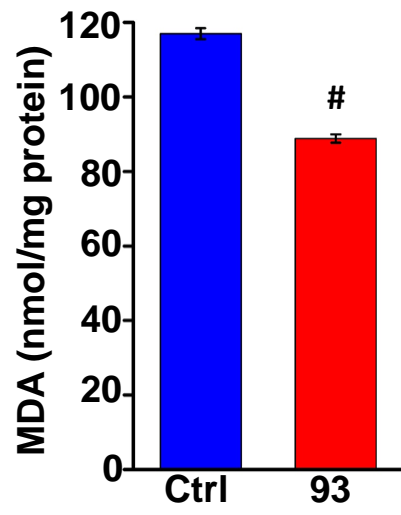
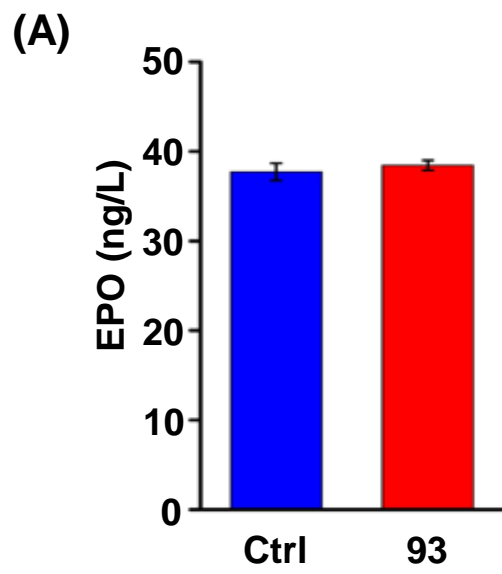


Figure S20

(A)





Supplemental References

1. Hou YL, Zhang SP, Wang L, et al. Estrogen regulates iron homeostasis through governing hepatic hepcidin expression via an estrogen response element. *Gene*. 2012;511(2):398-403.
2. Viatte L, Lesbordes-Brion JC, Lou DQ, et al. Deregulation of proteins involved in iron metabolism in hepcidin-deficient mice. *Blood*. 2005;105(12):4861-4864.
3. Ramos E, Ruchala P, Goodnough JB, et al. Minihepcidins prevent iron overload in a hepcidin-deficient mouse model of severe hemochromatosis. *Blood*. 2012;120(18):3829-3836.
4. Wu Q, Wang H, An P, et al. HJV and HFE Play Distinct Roles in Regulating Hepcidin. *Antioxid Redox Signal*. 2015;22(15):1325-1336.
5. Yang B, Kirby S, Lewis J, Detloff PJ, Maeda N, Smithies O. A mouse model for beta 0-thalassemia. *Proc Natl Acad Sci U S A*. 1995;92(25):11608-11612.
6. Zhang M, Liu J, Guo WL, Liu X, Liu SJ, Yin HJ. Icaritin regulates systemic iron metabolism by increasing hepatic hepcidin expression through Stat3 and Smad1/5/8 signaling. *Blood*. 2016;37(5):1379-1388.
7. Zhang S, Chen Y, Guo W, et al. Disordered hepcidin-ferroportin signaling promotes breast cancer growth. *Cell Signal*. 2014;26(11):2539-2550.
8. Dragatsis I, Efstratiadis A, Zeitlin S. Mouse mutant embryos lacking huntingtin are rescued from lethality by wild-type extraembryonic tissues. *Development*. 1998;125(8):1529-1539.
9. Liu J, Zhang J, Ginzburg Y, et al. Quantitative analysis of murine terminal erythroid differentiation in vivo: novel method to study normal and disordered erythropoiesis. *Blood*. 2013;121(8):e43-49.